Uncertainty Spillovers in Central America: A Quantile Connectedness Approach

Roberto McLean Ponce

Independent Researcher, Nicaragua

roberto.mclean2819@gmail.com

July 2026

Abstract

How does macroeconomic uncertainty propagate across small open emerging economies, and does transmission intensify when uncertainty is extreme? We examine seven Central American and Caribbean economies and the United States using country-specific Macroeconomic Uncertainty Indices and a Quantile VAR connectedness framework over 1995:05–2025:12. We find strong nonlinearities in regional uncertainty spillovers. At a one-month horizon, total connectedness rises from 26.5% at the median to 94.0% in the upper tail, a 3.5-fold increase during episodes of exceptionally high uncertainty. This amplification persists at longer horizons, although the structure of transmission changes substantially. The United States and Honduras are persistent net transmitters, while Panama and the Dominican Republic are major short-horizon receivers. Nicaragua, in contrast, shifts from a modest net receiver at one month to the system's second-largest net transmitter at twelve months in the upper tail. These findings are robust to an independently coded quantile-VAR estimator and block-bootstrap inference. An orthogonalisation exercise further shows that removing contemporaneous US exposure leaves 98.6% of upper-tail connectedness intact. Overall, uncertainty spillovers across small open emerging economies are highly nonlinear and horizon-dependent, becoming substantially stronger precisely when uncertainty is most extreme.

Keywords: Macroeconomic uncertainty, quantile VAR, CAPRD, tail risk, spillovers.

JEL codes: C32, E32, E44, F41, O54.

Acknowledgments and Disclosure. This research received no external financial support. The author declares no financial relationships or other potential conflicts of interest relevant to this research.

Contents

1 Introduction **4**

2 Literature Review **8**

3 Methodology **13**

3.1 Overview . . . 13

3.2 Stage 1: Measuring Country-Level Macroeconomic Uncertainty . . . 13

3.2.1 Conceptual framework . . . 13

3.2.2 Data and panel construction . . . 14

3.2.3 Factor extraction under missing data . . . 15

3.2.4 Individual forecast models . . . 15

3.2.5 Stochastic volatility estimation . . . 16

3.3 Stage 2: Quantile Connectedness Analysis . . . 16

3.3.1 The Diebold–Yilmaz connectedness framework . . . 16

3.3.2 The Quantile VAR . . . 17

3.3.3 VAR specification . . . 18

3.3.4 Dynamic rolling connectedness . . . 18

3.4 Pre-Estimation Diagnostics . . . 18

3.5 Identification and Limitations . . . 19

3.6 Software and Replication . . . 20

4 Data: Constructing the CAPRD Uncertainty Indices **21**

4.1 What the Peaks Are: Five Major Episodes per Country . . . 22

4.2 Do the Factors Actually Capture Common Variation? . . . 28

5 Results **30**

5.1 Tier 1: The MUI Series and Their Within-Country Structure . . . 30

5.1.1 Pre-estimation diagnostics . . . 30

5.1.2 Within-country variance structure . . . 31

5.2 Tier 1.5: Country-Level Real Effects of Uncertainty . . . 32

5.2.1 Recursive VAR evidence . . . 32

5.2.2 Quantile regression evidence: where in the growth distribution does uncertainty bind? . . . 35

5.3 Tier 2: QVAR Connectedness, The Network Architecture . . . 39

5.3.1 The central result: tail amplification . . . 39

5.3.2 Who transmits and who receives . . . 40

5.3.3 The network visualised . . . 42

5.3.4 Dynamic connectedness, how the network moves through time . 44

5.3.5 The horizon dimension . . . 48

5.4 Tier 3: Verification Exercises 48
5.4.1 Is the tail amplification distinguishable from sampling noise? . . 48
5.4.2 Is the upper-tail TCI a mechanical consequence of a shared US factor? 49

6 Discussion **50**

7 Conclusion **52**

A Appendix: MUI Construction Data **53**
A.1 Additional Country-Level VAR Impulse Responses 56

1 Introduction

Uncertainty is a word economics borrowed and then had to discipline. Frank Knight (1921) drew the boundary a century ago. Risk is variation whose probability distribution is known or estimable. Uncertainty is variation for which even the space of outcomes resists enumeration. That distinction is uncomfortable for an empirical discipline built on variances and confidence intervals, and the modern literature on macroeconomic uncertainty is, in essence, a century-long attempt to build measurable proxies for a genuinely Knightian object without pretending the gap has been closed. Financial-market volatility indices price near-term risk, as does the VIX. Text-mining approaches count the newsprint frequency of uncertainty-related terms, as in the Economic Policy Uncertainty (EPU) index of Baker et al. (2016) and its global extension, the World Uncertainty Index. Survey-based measures extract the cross-sectional dispersion of professional forecasts (Rossi and Sekhposyan, 2015). Each of these is a reasonable proxy, and each conflates genuine unforecastability with something else, whether realised volatility, media attention, or forecaster disagreement driven by heterogeneous information rather than by fundamental unpredictability.

Jurado et al. (2015) close much of that gap by defining macroeconomic uncertainty directly as the conditional volatility of the purely unforecastable component of a large panel of economic series. The object is not how much a variable moves, but how much of that movement could not have been anticipated given everything knowable at the time. Bloom (2009) and, earlier, Pindyck (1991); Bloom et al. (2007) give this construct its behavioural content. Because investment is frequently irreversible, a rise in uncertainty raises the option value of waiting and generates a synchronised, economy-wide pause in hiring and capital spending that need not depend on any change in the expected return of any single project. Bloom (2014) and Ludvigson et al. (2021) show that this mechanism is not confined to the conditional mean of the uncertainty process. The tails of the distribution, the months of genuinely extraordinary uncertainty, carry a disproportionate share of the real effects. That observation is the methodological premise of this paper. If uncertainty's consequences concentrate in its tails, then a network of cross-country uncertainty transmission estimated only at the conditional mean is, by construction, looking in the wrong place for the moments that matter most.

The transmission dimension of the uncertainty literature developed largely in parallel. Diebold and Yilmaz (2009, 2012) recast the forecast-error-variance decomposition of a VAR as a connectedness network, identifying who transmits and who receives shocks across a system of variables or countries. Antonakakis et al. (2018) and Gabauer and Gupta (2018) apply this to cross-country uncertainty and EPU transmission and find a systematically dominant US role, a pattern echoed in the broader evidence on

cross-border policy-uncertainty spillovers assembled by Biljanovska et al. (2021) and, for Latin America specifically, by Ghirelli et al. (2021) and Andres-Escayola et al. (2025). Within Central America itself, Urbina and Marenco (2024) build a Diebold-Yilmaz interconnectivity index from each country's Monthly Economic Activity Index and show that it tracks the pace of regional economic integration closely enough to date its accelerations and its slowdowns, while identifying which economies act as net emitters and which as net receivers of integration impulses over time. McLean et al. (2024) take the same forecast-error-variance logic to a different variable, estimating a generalised VAR for CAPRD inflation and its main trading partners over 2000 to 2023 and showing that oil-price shocks and the Global Supply Chain Pressure Index explain a material share of the region's inflation dynamics. McLean (2026) goes further along the mean-based connectedness route, estimating a Bayesian Global VAR with stochastic volatility and a stochastic search variable selection prior on a nineteen-country panel, including all seven CAPRD economies, to trace how economic policy uncertainty originating in the United States and in China transmits into each recipient's own EPU index. That paper finds that US EPU shocks are the dominant bilateral source of uncertainty for most CAPRD economies, that China registers a smaller bilateral footprint on most individual CAPRD recipients but a substantial system-wide one once contributions are aggregated across the full nineteen-country panel, and that this asymmetry survives both the exclusion of the COVID-19 period and a reduced twelve-country specification. These three papers confirm that CAPRD economies are densely linked through conventional macro-financial channels and that a VAR-based connectedness framework, whether classical, Bayesian, or global in scope, is well suited to measuring the linkage. None asks the question this paper asks. What these mean-based networks cannot show, by construction, is whether the architecture of transmission itself changes when uncertainty is at its most extreme, precisely the regime in which, per Bloom (2014), the economic stakes are highest.

Chatziantoniou et al. (2021) supply the tool that closes this second gap. They replace the OLS VAR underlying the connectedness framework with equation-by-equation quantile regressions, so that the resulting Quantile VAR (QVAR) yields a distinct connectedness table for the median, for calm periods, and for periods of acute stress. Applied to interest-rate swaps, they find upper-tail connectedness exceeding the median by factors of two to four. Applied to disaggregated JLN uncertainty sub-indices by Ben Haddad et al. (2024), the same widening shows up again. The tail is where the network tightens.

The empirical space this paper occupies combines that methodological point with a specific regional setting that has not, to our knowledge, been examined through it. The seven Central America, Panama, and Dominican Republic (CAPRD) economies are small, open, and bound to the United States through trade, remittances, and,

in two cases, dollarisation, yet they are far from a homogeneous bloc. Dollarised and non-dollarised monetary regimes sit side by side. Commodity-dependent and services-and-remittance-dependent economies share the same dominant trade partner. Idiosyncratic domestic uncertainty, from political crises to natural disasters to security shocks, coexists with a common external exposure to US and global conditions, so that whether CAPRD uncertainty travels mainly from the United States inward, circulates within the region, or does both depending on how extreme conditions are, is a genuine empirical question rather than a foregone conclusion. The thirty-year sample used here spans stress episodes of markedly different character, including Hurricane Mitch in 1998, the 2008 to 2009 Global Financial Crisis, Nicaragua's 2018 socio-political crisis, and the COVID-19 pandemic, which lets us ask whether uncertainty connectedness is a stable structural feature of the region or whether it reconfigures itself episode by episode. Diakonova et al. (2025) and Molina et al. (2023) establish that uncertainty is a first-order, measurable phenomenon within the CAPRD using EPU-style proxies, and Urbina and Marenco (2024) confirm that the region's economies move together closely enough for a connectedness index built on real activity to track integration itself. None of this work quantifies a distribution-dependent network of uncertainty transmission across the CAPRD bloc, and none asks whether that network's tail behaviour differs from its typical-month behaviour. Answering that question requires the theoretically disciplined MUI measure of Jurado et al. (2015), built country by country for all seven economies and the United States, run through the quantile connectedness framework of Chatziantoniou et al. (2021).

Accordingly, the paper does three things. First, it constructs country-specific MUI series for all seven CAPRD economies and the United States following the Jurado et al. (2015) methodology, using country-tailored panels of forty to more than one hundred and thirty macro-financial series per economy spanning activity, prices, money, banking, the public sector, external accounts, interest rates, and, where available, FX, energy, and labour-market indicators. Second, it estimates the full QVAR connectedness network for this eight-economy system across three quantiles ($\tau = 0.05, 0.50, 0.95$) and three forecast horizons ($h = 1, 3, 12$ months), documenting who transmits, who receives, and how that architecture shifts between calm and stress regimes and across the horizon. Third, it subjects the resulting network to an independent verification using a separately coded quantile-VAR estimator and a US-orthogonalisation exercise, asking directly whether the tail connectedness documented here survives sampling variation and whether it is a mechanical consequence of shared exposure to US uncertainty rather than genuine cross-country linkage. Throughout, the framing is deliberately narrow. The estimates that follow are reduced-form, quantile-conditional forecast-error variance decompositions for this sample, this set of countries, and this period. They document how much of one

country's uncertainty forecast error is statistically attributable to shocks elsewhere in the network under a given uncertainty regime. They are not evidence of a structural transmission mechanism, and they carry no policy prescription. What the data show is that CAPRD uncertainty connectedness rises sharply when the region moves from its typical month to its ninety-fifth-percentile month, and that finding, on its own terms, is the contribution of this paper.

The remainder of the paper proceeds as follows. Section 2 reviews the measurement and transmission literatures in more detail. Section 3 sets out the two-stage empirical strategy, first MUI construction, then QVAR connectedness. Section 4 describes the resulting indices, the data blocks that feed them, and their historical peaks. Section 5 presents the results in three tiers, the MUI series themselves and their within-country variance structure, the static and dynamic QVAR connectedness network, and a set of verification exercises targeted at the network's most policy-relevant features. Section 6 discusses what the findings suggest and what they leave open, and Section 7 concludes.

2 Literature Review

The Nature and Measurement of Macroeconomic Uncertainty

The economics literature has grappled for decades with the distinction between risk — probabilistic variation over known outcomes — and genuine uncertainty, which Knight (1921) famously characterised as unquantifiable ignorance. Modern macroeconomics has operationalised this distinction through a proliferation of empirical proxies that differ substantially in their theoretical foundations and empirical properties. Financial volatility indices such as the VIX capture the market's priced expectation of near-term equity volatility, while news-based measures like the Economic Policy Uncertainty (EPU) index of Baker et al. (2016) count the frequency of uncertainty-related terms in newspaper archives. Survey-based disagreement measures extract cross-sectional dispersion in professional forecasters' expectations as a proxy for uncertainty about the future path of the economy (Rossi and Sekhposyan, 2015). Each of these approaches conflates genuine uncertainty with realised volatility or with disagreement driven by heterogeneous information sets rather than fundamental unpredictability. The World Uncertainty Index of Ahir et al. (2022) extends the text-mining approach globally across 143 countries, providing a first cross-country view but inheriting the same conceptual limitations.

The measurement framework that most directly addresses the theoretical requirement of unpredictability is that of Jurado et al. (2015), who define macroeconomic uncertainty as the conditional volatility of the purely unforecastable component of a large set of economic indicators. This is a fundamentally different object from the volatility of the indicators themselves: a series can be highly variable yet perfectly predictable, in which case it contributes nothing to genuine uncertainty. As Ludvigson et al. (2021) show, this distinction has first-order empirical consequences — the JLN uncertainty measure identifies far fewer but substantially larger uncertainty episodes than EPU or VIX-based proxies, and its effects on economic activity are correspondingly more persistent. Cascaldi-Garcia et al. (2023), in an authoritative survey of the literature, conclude that the JLN methodology represents the current frontier in macroeconomic uncertainty measurement precisely because it operationalises the theoretically correct concept rather than a proxy that happens to be observable. Building directly on this framework, Ben Haddad et al. (2024) recently showed that disaggregating the JLN measure into sub-indices and examining cross-index spillovers via quantile VAR connectedness reveals asymmetric transmission patterns that are invisible at the aggregate level — a finding that motivates our cross-country application of the same methodology.

Uncertainty, Investment, and the Business Cycle

The real effects of uncertainty have been theorised through multiple channels. The real options theory, developed by Bloom et al. (2007) and extended in the landmark study of Bloom (2009), predicts that irreversible investment decisions are postponed in high-uncertainty environments because the option value of waiting is higher than the net present value of immediate commitment. This mechanism generates a "wait-and-see" pause in economic activity that is simultaneously contractionary and swift: uncertainty shocks produce sharp short-run contractions followed by sharp rebounds as the fog lifts. Stochastic volatility models estimated by Fernández-Villaverde et al. (2015) extend this reasoning to fiscal policy, showing that uncertainty about the composition and timing of fiscal consolidation generates output contractions comparable in magnitude to a 25-basis-point monetary tightening. Bloom (2014) provides a comprehensive survey of these mechanisms, documenting that uncertainty episodes consistently predict business cycle downturns across a wide range of countries and measurement approaches, and that higher-order moments of the uncertainty distribution — the tails — tend to dominate the conditional mean in explaining output dynamics. This last point is particularly relevant for our study: if tail uncertainty matters more than average uncertainty, then the quantile VAR approach we employ is not merely a robustness exercise but a methodologically essential tool for capturing the relevant dynamics.

Uncertainty in Small Open and Developing Economies

The effects of uncertainty documented for large advanced economies do not translate straightforwardly to small open developing economies, where additional transmission channels and structural vulnerabilities alter both the magnitude and the persistence of uncertainty shocks. Small open economies face exogenous external uncertainty shocks that are beyond domestic policy influence, yet must respond to them with limited monetary and fiscal space. Calderón and Fuentes (2014) document that business cycle synchronisation in Latin America with the United States is substantial and has increased over time, creating a transmission belt for US uncertainty shocks. The IMF (2022; 2024) has quantified these external spillovers, showing that US monetary tightening — itself partly driven by uncertainty about the inflation path — generates contractionary effects in Latin America that are amplified in countries with higher external debt, tighter financial conditions, and weaker institutional frameworks.

Within the CAPRD specifically, Diakonova et al. (2025) construct text-based economic policy uncertainty indices for all seven countries using a Spanish-language newspaper corpus, providing the first systematic documentation of country-level EPU dynamics in the region. They find that domestic uncertainty in the CAPRD co-moves substantially with US EPU but also exhibits country-specific components driven by electoral cycles,

fiscal consolidation episodes, and natural disasters. Complementarily, Molina et al. (2023) analyse political uncertainty in Latin America using textual data and find that governance fragility amplifies the economic impact of external uncertainty shocks, a feature particularly salient in countries like Nicaragua and Honduras where political risk premia are structurally elevated. These papers establish the relevance of uncertainty as an object of study in the CAPRD, but stop short of quantifying the dynamic network of uncertainty transmission across countries — precisely the gap our paper fills.

Uncertainty Spillovers: Methodology and Evidence

The connectedness framework of Diebold and Yilmaz (2009, 2012, 2014), which decomposes forecast error variance into own-variance and cross-variance contributions via generalised impulse response functions (Pesaran and Shin, 1998; Koop et al., 1996), has become the workhorse methodology for quantifying directional spillovers across a network of variables. Its application to uncertainty transmission was pioneered by Antonakakis et al. (2018), who showed that uncertainty connectedness across G7 economies is highly time-varying, spiking during the Global Financial Crisis and at geopolitical stress events but declining during tranquil periods. Gabauer and Gupta (2018) extended this to cross-country transmission of EPU shocks and found that the United States is systematically a net transmitter of uncertainty to other economies, consistent with the dominant role of US monetary and fiscal policy in global financial conditions.

A critical limitation of these mean-based connectedness measures is that they characterise dynamics at the centre of the distribution and may miss the most important non-linearities — precisely those that emerge during extreme events. Chatziantoniou et al. (2021) address this by replacing the conventional OLS VAR with equation-by-equation quantile regressions, yielding a Quantile VAR (QVAR) that produces distribution-specific connectedness tables. Their empirical application to interest rate swaps shows that upper-tail connectedness — relevant during stress periods — can exceed median connectedness by factors of two to four, revealing a non-linear amplification mechanism that mean-based models systematically understate. Ben Haddad et al. (2024) apply this framework directly to the JLN uncertainty sub-indices and find that financial uncertainty is the dominant transmitter to real activity at the upper tail, while macroeconomic uncertainty drives real outcomes across all quantiles — a decomposition that informs how we interpret cross-country uncertainty transmission when different CAPRD economies specialise in different sectors.

For Latin America specifically, Ghirelli et al. (2021) document significant spillovers from Latin American EPU to the Spanish economy, exploiting the close trade, financial, and cultural ties between Spain and the region. Using a structural VAR with sign

restrictions, they find that uncertainty shocks originating in Brazil, Mexico, Argentina, and Chile generate measurable output contractions in Spain, with the transmission operating primarily through trade and financial channels rather than through direct contagion. The companion working paper Ghirelli et al. (2020) and the more recent study by Andres-Escayola et al. (2025) extend this analysis, finding that the direction of spillovers is asymmetric and time-varying: US uncertainty transmits strongly to Latin America, while the reverse direction is weaker and operates mainly during global crises. Biljanovska et al. (2021) corroborate these findings across a broader sample, showing that economic policy uncertainty in large economies exerts significant "fear thy neighbour" effects on trading partners, with the magnitude proportional to trade exposure. For the CAPRD, where the US accounts for between 35 and 60 per cent of total exports across the seven economies, these findings suggest that external uncertainty transmission channels are likely to be substantial.

Regional Context: Prior Work on the CAPRD

Prior econometric work on macroeconomic dynamics within the CAPRD has focused primarily on business cycle synchronisation, inflation dynamics, and the real effects of remittances, rather than on uncertainty per se. McLean et al. (2024) examine inflation spillovers across the CAPRD and find that global commodity price shocks transmit rapidly and symmetrically across countries, while domestic price pressures exhibit more heterogeneous dynamics that reflect country-specific monetary frameworks and exchange rate regimes. McLean (2026) extends this analysis to economic policy uncertainty, using a Bayesian Global VAR to document that US and Chinese EPU shocks generate heterogeneous contractionary effects across CAPRD economies, with dollarised economies facing a more direct transmission through credit channels while countries with managed exchange rates exhibit more muted short-run impacts but larger persistent effects. The broader integration dynamics of the CAPRD region are examined by Urbina and Marenco (2024), who apply a time-varying connectedness approach to document that intra-regional economic integration has deepened since 2010 but remains asymmetric, with Nicaragua and Honduras more exposed to uncertainty originating in Guatemala and Costa Rica than the reverse. Urbina (2013) provides an earlier baseline for financial spillovers across Central America using variance decomposition methods, finding that financial shocks in the larger economies rapidly contaminate smaller ones.

Taken together, this literature establishes three facts that motivate our paper. First, macroeconomic uncertainty is a quantifiable and economically important phenomenon that requires careful measurement beyond simple volatility proxies, and the JLN framework is the current state of the art. Second, uncertainty transmits across borders in directional, asymmetric, and non-linear ways, with the tails of the distribution

exhibiting substantially larger spillovers than the conditional mean suggests — a feature the QVAR connectedness methodology is specifically designed to capture. Third, the CAPRD region is deeply embedded in the global uncertainty network through its exposure to the US, yet its internal uncertainty dynamics and the direction of intra-regional transmission remain essentially undocumented. Our contribution is to close this gap by constructing country-specific JLN indices for all seven CAPRD economies and the United States, and estimating the full quantile connectedness network across the distribution of uncertainty. Rather than asking simply whether uncertainty spillovers exist — they do — we ask whether the region amplifies or attenuates these spillovers at the upper tail, and which economies bear the burden of receiving versus transmitting uncertainty shocks during periods of extreme stress.

3 Methodology

3.1 Overview

This paper adopts a two-stage empirical strategy. Our work contributes to a growing literature on uncertainty measurement and spillovers in Central America and the CAPRD region (McLean, 2026; McLean et al., 2024; Urbina and Marenco, 2024; Diakonova et al., 2025; Ghirelli et al., 2021; Andres-Escayola et al., 2025). In the first stage, we construct country-specific Macroeconomic Uncertainty Indices (MUI) for seven CAPRD economies — Costa Rica, Dominican Republic, El Salvador, Guatemala, Honduras, Nicaragua, and Panama — as well as for the United States, following the factor-based econometric framework of Jurado et al. (2015). In the second stage, we quantify the cross-country transmission of uncertainty shocks using the Quantile Vector Autoregression (QVAR) connectedness methodology of Chatziantoniou et al. (2021), as implemented in the `ConnectednessApproach` R package of Gabauer (2022). This two-stage design separates the measurement problem — which requires country-level panel data that are both large (N) and long (T) — from the transmission problem, which is inherently multi-country and benefits from distributional flexibility offered by quantile methods.

3.2 Stage 1: Measuring Country-Level Macroeconomic Uncertainty

3.2.1 Conceptual framework

Economic uncertainty is fundamentally unobservable. The literature has proposed diverse proxies, including stock market volatility (Bloom, 2009), text-based news indices (Baker et al., 2016), cross-sectional dispersion measures (Backus and Zin, 1994), and survey disagreement (Rossi and Sekhposyan, 2015). Each proxy conflates genuine uncertainty with variation in measurable outcomes, potentially misclassifying episodes of high volatility as uncertainty when they are simply realised risk.

Jurado et al. (2015) (henceforth JLN) provide a direct econometric estimate of macroeconomic uncertainty that circumvents this identification problem. Their key insight is that the uncertainty facing agent i at time t about variable y_{it+h} is the conditional volatility of the unforecastable component of y_{it+h}:

$$U_{it}^{y}(h) \;=\; \sqrt{\mathbb{E}\Big[\big(y_{it+h} - \mathbb{E}[y_{it+h} \mid \mathcal{I}_t]\big)^2 \mid \mathcal{I}_t\Big]}, \tag{1}$$

where $\mathcal{I}_t$ is the information set at time t and h is the forecast horizon. Rather than measuring the volatility of y_{it} itself, JLN measure the volatility of its *purely*

unforecastable component — a conceptually distinct and more demanding notion of uncertainty. As Ludvigson et al. (2021) emphasise, this distinction matters empirically: the quantitatively important uncertainty episodes implied by the JLN measure appear far less frequently but are much larger and more persistent than popular proxies suggest.

The aggregate MUI is then the average across N series of the h-step-ahead individual uncertainties:

$$U_t^{\mathcal{M}}(h) \;=\; \frac{1}{N}\sum_{i=1}^{N} U_{it}^{y}(h), \tag{2}$$

standardised to have unit mean over the full sample. We construct indices at horizons $h \in \{1, 3, 12\}$ months, following the original JLN specification. The $h = 1$ index captures current uncertainty about the near-term macroeconomic environment; $h = 3$ captures medium-run uncertainty; and $h = 12$ captures longer-run structural uncertainty.

3.2.2 Data and panel construction

For each CAPRD country, we compile an unbalanced monthly panel of macroeconomic series spanning prices, activity, money, credit, interest rates, public finances, and trade. Series counts range from 107 (Dominican Republic) to 141 (Guatemala), reflecting differences in data availability across the region. All series are seasonally adjusted where indicated using a rolling ratio-to-moving-average procedure with a 10-year centred window, which captures the evolution of seasonal patterns over the three-decade sample without imposing a single fixed factor.[1] Series are subsequently transformed to stationarity using the transformation codes of Stock and Watson (2002): log-differences (`tcode` 5) for price, quantity, and monetary series; first differences (`tcode` 2) for series with negative values such as fiscal balances; and levels (`tcode` 1) for interest rates and expectations, which are already stationary.

The unbalanced structure of the panels — with older series starting as far back as 1990 and newer series beginning in the 2000s or 2010s — is handled by treating missing observations as genuinely unobserved rather than as zeros. Factor estimation and individual forecast models (see below) operate on the available observations for each series, so later entrants contribute information only from their own start date onward. The aggregate MUI in (2) uses a cross-sectionally normalised average that corrects for level shifts when new series join the panel, as proposed implicitly by Jurado et al. (2015)

[1] Fixed-sample seasonal factors — the standard approach in the classical decomposition — systematically under-adjust series whose seasonal patterns evolve over time, leaving residual seasonality in the transformed data. For multi-step uncertainty measures ($h = 3$, $h = 12$), this residual is amplified because (1) aggregates the latent log-vol state h_t across several consecutive months, so end-of-year spikes in h_t appear in both December and January of the MUI, generating a characteristic double-peak. The rolling window correction removes this artefact while preserving higher-frequency variation.

and formalised in our implementation as:

$$U_t^{\mathcal{M},\text{norm}}(h) \;=\; \frac{1}{N_t} \sum_{i:\, t \geq t_{0i}} \frac{U_{it}^{y}(h)}{\bar{U}_i^{y}(h)}, \tag{3}$$

where N_t is the number of series available at t and $\bar{U}_i^{y}(h)$ is the time-series mean of series i's uncertainty. Equation (3) is the headline series reported in all tables and figures; the raw cross-sectional average (2) is retained as a robustness comparison.

The US uncertainty index is taken directly from Jurado et al. (2015) as updated through the Federal Reserve Bank of St. Louis FRED database (Jurado et al., 2024).

3.2.3 Factor extraction under missing data

Individual forecast models require common factors extracted from the full unbalanced panel. We apply the Expectation-Maximisation Principal Components Analysis (EM-PCA) of Stock and Watson (2002), which iterates between (i) imputing missing values given the current factor estimates and (ii) updating factor estimates via standard PCA on the completed data, until convergence. Formally, denoting the balanced completion at iteration s as $\tilde{\mathbf{X}}^{(s)}$, the EM step solves:

$$\hat{\mathbf{F}}^{(s+1)} = \text{PC}_r\left(\tilde{\mathbf{X}}^{(s)}\right), \tag{4}$$

$$\tilde{x}_{it}^{(s+1)} = \hat{\lambda}_i^{(s+1)\prime} \hat{f}_t^{(s+1)} \quad \text{for all } (i,t) \text{ with } x_{it} \text{ missing}, \tag{5}$$

where $\text{PC}_r(\cdot)$ extracts the leading r principal components and $\hat{\lambda}_i$ is the corresponding factor loading. The number of factors r is selected by the IC_{p2} criterion of Bai and Ng (2002). As a robustness check, we verify that EM-PCA on a balanced sub-sample reproduces standard PCA up to sign normalisation, and that the full-panel factor estimates are highly correlated with those from the balanced sub-sample over their common period.

3.2.4 Individual forecast models

The expected value $\mathbb{E}[y_{it+h} \mid \mathcal{I}_t]$ is estimated from a factor-augmented autoregressive model:

$$y_{it+h} \;=\; \mu_i + \sum_{j=1}^{p} \phi_{ij} y_{it-j+1} + \sum_{k=1}^{r_i} \gamma_{ik} f_{kt} + \varepsilon_{it+h}, \tag{6}$$

where f_{kt} are the estimated common factors and $p = 4$ lags throughout, following JLN. The number of factors $r_i \in \{0, \ldots, r\}$ included for series i is selected by AIC applied to each individual model. A series with $r_i = 0$ reduces to a pure AR(4) model. The stochastic volatility of the residual ε_{it+h} — which defines the uncertainty measure (1) — is estimated by Markov Chain Monte Carlo (MCMC) using the `stochvol` package

(Kastner, 2016) in R, drawing 50 000 posterior samples after 50 000 burn-in iterations with thinning factor 10.

3.2.5 Stochastic volatility estimation

The residual log-variance follows a latent AR(1) process:

$$\varepsilon_{it} = \exp(h_{it}/2)\,\eta_{it}, \quad \eta_{it} \sim \mathcal{N}(0,1), \tag{7}$$

$$h_{it} = \mu_i + \phi_i(h_{it-1} - \mu_i) + \sigma_i \xi_{it}, \quad \xi_{it} \sim \mathcal{N}(0,1), \tag{8}$$

with $|\phi_i| < 1$ ensuring stationarity of the log-variance process. The posterior means $\hat{\mu}_i$, $\hat{\phi}_i$, $\hat{\sigma}_i$, and $\{\hat{h}_{it}\}_{t=1}^{T}$ are obtained from the MCMC sampler. Convergence is assessed by Geweke (1992) z-statistics on the sampled parameters.[2] Posterior uncertainty about h_{it} propagates directly to the MUI through (1), so our aggregate index inherits a measure of estimation uncertainty that standard proxies ignore.

3.3 Stage 2: Quantile Connectedness Analysis

3.3.1 The Diebold–Yilmaz connectedness framework

The connectedness approach of Diebold and Yilmaz (2012) decomposes the H-step-ahead generalised forecast error variance of a system of n variables into own-variance and cross-variance components. Consider an n-dimensional VAR(p) for the vector $\mathbf{x}_t = (x_{1t}, \ldots, x_{nt})'$:

$$\mathbf{x}_t \;=\; \sum_{\ell=1}^{p} \mathbf{\Phi}_\ell\, \mathbf{x}_{t-\ell} + \boldsymbol{\varepsilon}_t, \qquad \boldsymbol{\varepsilon}_t \sim (0, \mathbf{\Sigma}), \tag{9}$$

with moving-average representation $\mathbf{x}_t = \sum_{j=0}^{\infty} \mathbf{A}_j\, \boldsymbol{\varepsilon}_{t-j}$. Using the generalised identification scheme of Koop et al. (1996) and Pesaran and Shin (1998), which is invariant to variable ordering, the (i,j) element of the H-step-ahead generalised forecast error variance decomposition (GFEVD) is:

$$\theta^{g}_{ij}(H) \;=\; \frac{\sigma_{jj}^{-1} \sum_{h=0}^{H-1} \left(\mathbf{e}_i' \mathbf{A}_h \mathbf{\Sigma} \mathbf{e}_j\right)^2}{\sum_{h=0}^{H-1} \left(\mathbf{e}_i' \mathbf{A}_h \mathbf{\Sigma} \mathbf{A}_h' \mathbf{e}_i\right)}, \tag{10}$$

where $\mathbf{e}_i$ is the i-th unit selection vector and $\sigma_{jj} = (\mathbf{\Sigma})_{jj}$. Since rows of the GFEVD need not sum to unity under the generalised scheme, the normalised shares are $\tilde{\theta}^{g}_{ij}(H) = \theta^{g}_{ij}(H) / \sum_{j=1}^{n} \theta^{g}_{ij}(H)$.

[2] For series with $\hat{\phi}_i > 0.95$ (high persistence), the SV model implies that the log-variance is nearly non-stationary. We retain these series in the aggregate because the posterior mean remains well-defined and the Geweke diagnostic does not flag non-convergence; however, we confirm qualitative robustness by repeating the analysis with persistence-trimmed cross-sections.

The connectedness measures follow directly:

$$\text{Total Connectedness Index (TCI)} = \frac{\sum_{i \neq j} \tilde{\theta}^g_{ij}(H)}{n}, \tag{11}$$

$$\text{FROM}_i(H) = \frac{\sum_{j \neq i} \tilde{\theta}^g_{ij}(H)}{n}, \tag{12}$$

$$\text{TO}_j(H) = \frac{\sum_{i \neq j} \tilde{\theta}^g_{ij}(H)}{n}, \tag{13}$$

$$\text{NET}_i(H) = \text{TO}_i(H) - \text{FROM}_i(H). \tag{14}$$

A positive NET_i identifies economy i as a net *transmitter* of uncertainty shocks; a negative value indicates a net *receiver*. Pairwise net transmission from j to i is $\text{NET}_{ij}(H) = \tilde{\theta}^g_{ji}(H) - \tilde{\theta}^g_{ij}(H)$.

3.3.2 The Quantile VAR

A critical limitation of the conventional DY framework is that the estimated VAR in (9) characterises only the *conditional mean* dynamics of $\mathbf{x}_t$. During stress periods — precisely when uncertainty is most consequential for policy — the relevant dynamics may differ substantially from mean behaviour. Chatziantoniou et al. (2021) extend the DY framework to the full conditional distribution by replacing the standard OLS estimator with a system of quantile regressions, one for each equation. For quantile $\tau \in (0, 1)$, the QVAR is:

$$Q_\tau(x_{it} \mid \mathbf{x}_{t-1}, \ldots, \mathbf{x}_{t-p}) \;=\; \alpha_i(\tau) + \sum_{\ell=1}^{p} \boldsymbol{\beta}_{i\ell}(\tau)' \, \mathbf{x}_{t-\ell}, \tag{15}$$

where $Q_\tau(\cdot \mid \cdot)$ denotes the τ-th conditional quantile and the coefficient vectors $\boldsymbol{\beta}_{i\ell}(\tau)$ are estimated by minimising the asymmetric absolute-loss function (check function):

$$\min_{\boldsymbol{\beta}} \sum_{t=1}^{T} \rho_\tau \left(x_{it} - \alpha_i(\tau) - \sum_{\ell=1}^{p} \boldsymbol{\beta}_{i\ell}(\tau)' \mathbf{x}_{t-\ell} \right), \tag{16}$$

where $\rho_\tau(u) = u[\tau - \mathbf{1}(u < 0)]$ is the Koenker and Bassett (1978a) check function. Once the quantile-specific coefficient matrices $\hat{\boldsymbol{\Phi}}_\ell(\tau)$ are obtained, the GFEVD in (10) is computed from the quantile MA representation and the connectedness measures follow exactly as in equations (11)–(14). This delivers τ-specific connectedness tables and dynamic indices.

We estimate the QVAR at three quantiles: $\tau \in \{0.05, 0.50, 0.95\}$. The median ($\tau = 0.50$) replicates the mean-based DY results under symmetric error distributions, providing a benchmark. The lower quantile ($\tau = 0.05$) identifies connectedness during *crisis* or *extreme low-uncertainty* periods, when uncertainty is surprisingly low — a situation

that can reflect abnormal calm before a sudden reversal (Chatziantoniou et al., 2021). The upper quantile ($\tau = 0.95$) is of primary interest: it captures connectedness during episodes of *extreme high uncertainty*, such as the 2008–09 Global Financial Crisis, the 2018 Nicaraguan socio-political crisis, and the 2020 COVID-19 pandemic. If upper-tail connectedness exceeds median connectedness, the region exhibits *tail amplification* — spillovers are more severe precisely when they are most damaging to economic activity.

3.3.3 VAR specification

Our system contains $n = 8$ variables: the $\text{MUI}_{h=1}$ indices for the seven CAPRD economies and for the United States. The common sample runs from May 1995 to December 2025 ($T = 368$ monthly observations), determined by Guatemala's data availability. All series are the entry-corrected normalised CSA measure in (3) and have been post-processed to remove residual seasonality in the MUI output using the ratio-to-moving-average method described in Section 3.2.2.

We set $p = 2$ lags following the Akaike Information Criterion (AIC) and Bayesian Information Criterion (BIC); both criteria select $p = 2$ for the baseline system. The forecast horizon for the GFEVD is $H = 12$ months, consistent with the common practice of Diebold and Yilmaz (2012) and subsequent literature (Antonakakis et al., 2018; Chatziantoniou et al., 2021). The main analysis is conducted on the $h = 1$ MUI; robustness checks with the $h = 3$ and $h = 12$ MUI are presented as additional robustness analysis.

3.3.4 Dynamic rolling connectedness

To track how uncertainty connectedness evolves across the business cycle and across major shock episodes, we estimate rolling-window versions of the static connectedness tables using a window of 48 months (four years), advanced one month at a time. This window is sufficiently long to estimate the QVAR reliably (368 observations, rolling at 48-month width yields 320 windows) while sufficiently short to capture structural breaks and regime changes in uncertainty transmission — such as those induced by the Global Financial Crisis, the 2014–16 commodity price collapse, the 2018 Nicaraguan crisis, and the COVID-19 pandemic. The resulting time series of $\text{TCI}(\tau)$, $\text{FROM}_i(\tau)$, $\text{TO}_i(\tau)$, and $\text{NET}_i(\tau)$ are the main dynamic outputs of our analysis.

3.4 Pre-Estimation Diagnostics

Before proceeding to the QVAR estimation, we conduct the full battery of pre-estimation diagnostics recommended for connectedness analyses.

Descriptive statistics. We report means, standard deviations, minima, maxima, and selected quantiles (p_5, p_{25}, p_{50}, p_{75}, p_{95}) for all eight MUI series. Skewness and excess kurtosis are included to motivate the use of quantile methods: heavy tails in the uncertainty distribution imply that mean-based inference misses tail behaviour.

Unit root and stationarity tests. We apply four complementary tests: the Augmented Dickey-Fuller (ADF) test (Dickey and Fuller, 1979), the Phillips-Perron (PP) test (Phillips and Perron, 1988), the Kwiatkowski-Phillips-Schmidt-Shin (KPSS) test (Kwiatkowski et al., 1992), and the Elliott-Rothenberg-Stock (ERS) efficient test (Elliott et al., 1996). The MUI measures are constructed to be stationary by design — they are cross-sectional averages of conditional standard deviations, which are bounded and positive — but we verify stationarity empirically. The QVAR framework does not require cointegration-based estimation even if near-unit-root behaviour is present (Chatziantoniou et al., 2021).

Normality tests. We apply the Jarque-Bera test (Jarque and Bera, 1980) and the Shapiro-Wilk test to each MUI series. Rejection of normality (expected given the heavy-tailed nature of uncertainty) motivates quantile over mean-based inference, as the latter is efficient only under normality and becomes dominated by extreme observations under fat tails.

Correlation and cross-sectional dependence. We compute the full 8×8 Pearson correlation matrix and test for cross-sectional dependence using the Pesaran (2004) CD test. Significant CD confirms that common shocks simultaneously affect all countries, providing a rationale for studying systemic connectedness rather than bilateral spillovers in isolation.

Optimal lag selection. Lag order p is chosen by minimising AIC, BIC, and the Hannan-Quinn (HQ) criterion. We present results for $p = 2$ (selected by all three criteria for the baseline system) and verify qualitative robustness at $p = 1$ and $p = 3$.

3.5 Identification and Limitations

A standard criticism of GFEVD-based connectedness measures is that they do not impose causal identification: shocks are not orthogonalised and correlated innovations enter all equations simultaneously. In the DY framework, this is an intentional choice — the generalised scheme averages over orderings to achieve invariance — but it implies that the connectedness measures reflect predictive relationships rather than causal mechanisms (Diebold and Yilmaz, 2014). We interpret our results accordingly: a large $\tilde{\theta}^g_{ij}$ means that country j's uncertainty history is strongly predictive of forecast

error variance in country i, not necessarily that shocks in j *cause* uncertainty in i in a structural sense.

The choice of quantile also involves a trade-off: lower quantiles are estimated from fewer extreme observations and are therefore less precisely estimated, while higher quantiles are more relevant for policy but may be driven by single outlier events. We report standard errors for all quantile coefficients and assess the statistical significance of differences between quantile-specific connectedness measures.

Finally, the two-stage structure implies that the first-stage estimation error in the MUI is not propagated to the second-stage QVAR. The MUI series are treated as observed variables in the QVAR, introducing a generated-regressor problem. While Jurado et al. (2015) argue that the factor-based estimates are sufficiently precise for this purpose — the MUI standard errors are negligible relative to the signal — a formal two-step correction would require bootstrap inference, which we leave for future work.

3.6 Software and Replication

The first stage (MUI construction) is implemented in MATLAB R2025b and R 4.5 using the `stochvol` package (Kastner, 2016) and the `coda` package for MCMC convergence diagnostics. The second stage (QVAR connectedness) is implemented entirely in R using the `ConnectednessApproach` package of Gabauer (2022) with the `QVAR` function, which implements the method of Chatziantoniou et al. (2021). All figures are produced with `ggplot2` (Wickham, 2016). Replication code is available upon request from the corresponding author.

4 Data: Constructing the CAPRD Uncertainty Indices

Before turning to the connectedness estimates, it is worth dwelling on what actually enters each country's MUI, because the index is only as credible as the panel of series it summarises. Each of the eight country-level uncertainty indices is built from a country-tailored data panel rather than a common, mechanically identical set of series across countries. This is a deliberate choice. Data availability and economic structure both differ sharply across the CAPRD, and forcing a common panel would either strand the analysis at the lowest common denominator of data availability or silently drop information that is genuinely informative for a given economy. Table 9 in the Appendix reports, for each of the seven CAPRD countries, how many series enter the underlying panel from each of eight economic categories, namely activity, prices, money, banking, the public sector, external accounts, interest rates, and FX and risk, with Nicaragua's panel additionally including small climate and energy blocks and a labour block that reflect its country-specific data landscape.

The resulting panels range from ninety series for Panama, a panel dominated by banking, interest-rate, and price indicators that reflects its role as a dollarised financial hub, to more than one hundred and thirty for Guatemala and Honduras, whose panels are unusually external-accounts-heavy. Prices is the single largest category in aggregate across the region, with 209 series, followed by external accounts at 169 and activity at 103. That ordering is itself informative. It indicates that the panels which discipline each country's MUI are weighted toward the price and external blocks that these small, open, and partly dollarised economies are most exposed to, rather than toward the domestic real-activity indicators that would dominate a similar exercise for a large, closed economy. Each series is assigned a stationarity-inducing transformation code, whether level, first or second difference, log, or log-difference, and is seasonally adjusted where appropriate prior to transformation, following the JLN pipeline described in Section 3.

Figure 1 plots the resulting MUI for each of the seven CAPRD economies over their full available history, at all three horizons ($h = 1$, 3, 12 months) simultaneously. Two features are worth noting before the formal descriptive statistics in Section 5.1. First, the historical peaks cluster overwhelmingly around a recognisable set of regional and global stress episodes rather than occurring at arbitrary dates, a pattern explored in detail below. Second, the scale of these peaks differs enormously across countries. The Dominican Republic's 1998 peak reaches roughly 1.5 on the raw, pre-normalisation MUI scale, more than double Panama's typical peak of under 1.0, a heterogeneity that motivates the cross-sectional normalisation applied before the QVAR step in Eq. 3 of

the Methodology.



Figure 1: Macroeconomic Uncertainty Index, by Country, All Horizons
Raw (pre-normalisation) MUI at $h = 1$, 3, and 12 months, constructed following Jurado et al. (2015), full available history through 2025:12 for each country (sample start varies by country according to data availability, see Table 9). United States MUI is constructed separately from a comparable US-specific data source and is summarised in Table 3 rather than plotted here. Source: own calculations.

4.1 What the Peaks Are: Five Major Episodes per Country

Labelling a peak with a date is not, on its own, informative about why uncertainty rose. Table 1 identifies the five most prominent, well-separated peaks in each country's $h = 1$ MUI series and matches each to the contemporaneous economic or political event most plausibly responsible for it. Three regional patterns emerge from this exercise. First, four of the seven countries show a peak within a few months of Hurricane Mitch's landfall

in late October 1998 (Honduras and Nicaragua, the two countries Mitch struck hardest, along with Costa Rica and Panama, both of which were exposed to the broader 1997 to 1998 episode of Asian and Russian financial contagion that preceded the hurricane by only a few weeks). Second, every one of the seven countries shows its single highest, or one of its two highest, realisations in either 2008 to 2009 (the Global Financial Crisis) or April to May 2020 (the COVID-19 pandemic), confirming that these two episodes were genuinely global and genuinely synchronised shocks to CAPRD uncertainty, in contrast to the more country-specific episodes that fill out the remaining peaks. Third, several of the peaks are purely domestic events with no obvious regional or global counterpart, the Dominican Republic's 2003 banking crisis, Honduras's 2009 constitutional crisis, and Nicaragua's April 2018 socio-political crisis chief among them, and these domestic episodes are in several cases the single largest realisation in that country's entire history, larger even than the Global Financial Crisis or COVID-19.

Table 1: Five Major MUI Peaks per Country and Associated Events

Country	Peak	Associated event
Costa Rica	1996:02	Residual fiscal and confidence effects of the September 1994 collapse of Banco Anglo Costarricense, Costa Rica's oldest state bank, whose closure raised the 1995 public-sector deficit by roughly two points of GDP and triggered a multi-year legislative and judicial investigation.
	1998:09	Onset of the global emerging-market turmoil following Russia's August 1998 sovereign default and the associated flight from emerging-market risk, arriving weeks before Hurricane Mitch made landfall in the region.
	2008:07	Build-up to the Global Financial Crisis, compounded by the mid-2008 spike in international oil and food commodity prices.
	2020:04	COVID-19 pandemic and associated national lockdown.
	2022:08	Aftermath of the April to May 2022 Conti ransomware attack against Costa Rican government systems, which prompted a declaration of national emergency, compounded by the global inflation surge following Russia's invasion of Ukraine.
Dominican Rep.	1998:02	Regional financial contagion from the 1997 Asian financial crisis and its continuation into early 1998.

Continued on next page

Table 1 continued from previous page

Country	Peak	Associated event
	2000:12	Political transition following President Hipólito Mejía's August 2000 inauguration amid a deteriorating external terms-of-trade environment.
	2003:04	Government intervention of Banco Intercontinental (Baninter) on 7 April 2003 after the discovery of an off-books parallel banking fraud later estimated at over US$2 billion, roughly two-thirds of the national budget.
	2004:10	Continued fallout of the 2003 banking crisis, including the contagion to Bancrédito and Banco Mercantil, a depreciation of the peso, and inflation approaching 30 percent in the crisis's aftermath.
	2006:06	Post-crisis adjustment and the run-up to the March 2007 entry into force of the CAFTA-DR free trade agreement for the Dominican Republic.
Guatemala	1996:06	Final months of the negotiations leading to the December 1996 Peace Accords that ended the 36-year civil war.
	1997:12	Early implementation uncertainty following the Peace Accords.
	1999:08	Run-up to the November 1999 general election won by Alfonso Portillo.
	2002:01	Fiscal slippage and corruption scandals during the Portillo administration that strained relations with the IMF.
	2020:05	COVID-19 pandemic.
Honduras	1997:01	Pre-election uncertainty ahead of the November 1997 general election won by Carlos Flores.
	1998:09	Regional financial contagion immediately preceding Hurricane Mitch, which made landfall in Honduras on 29 October 1998 and became the country's deadliest natural disaster of the twentieth century.
	2000:05	Post-Mitch reconstruction period and negotiations over Highly Indebted Poor Countries (HIPC) debt relief.

Continued on next page

Table 1 continued from previous page

Country	Peak	Associated event
	2009:12	Constitutional crisis following the 28 June 2009 removal of President Manuel Zelaya, with the contested 29 November 2009 election and the 2 December 2009 congressional vote reaffirming his ouster falling within this window.
	2020:04	COVID-19 pandemic, shortly followed by Hurricanes Eta and Iota in November 2020.
Nicaragua	1997:06	Early months of President Arnoldo Alemán's administration and the associated policy transition.
	1999:08	Regional stress in the run-up to the 2000 municipal elections and continued post-Mitch reconstruction.
	2008:11	Global Financial Crisis.
	2018:06	Peak of the April 2018 socio-political crisis, triggered by contested social-security reforms and protests, the country's largest domestic political crisis in the sample.
	2020:04	COVID-19 pandemic.
Panama	1998:10	Regional financial contagion coinciding with Hurricane Mitch, alongside uncertainty over the final December 1999 handover of the Panama Canal from the United States.
	2002:11	Corruption scandals and a sharp growth slowdown during the Moscoso administration (2001 to 2002).
	2007:01	Early implementation of the Panama Canal expansion approved by referendum in October 2006, alongside its financing arrangements.
	2008:10	Global Financial Crisis.
	2010:04	Post-crisis recovery period amid a change in administration under President Ricardo Martinelli.
El Salvador	1997:04	Post-civil-war reconstruction period following the 1992 Peace Accords and the March 1997 legislative and municipal elections.
	1999:04	Run-up to the March 1999 presidential election won by Francisco Flores and early debate over monetary integration with the United States.

Continued on next page

Table 1 continued from previous page

Country	Peak	Associated event
	2008:10	Global Financial Crisis.
	2020:04	COVID-19 pandemic.
	2023:09	Continuation of the state of exception against gangs in effect since March 2022 and the political run-up to President Nayib Bukele's disputed bid for re-election.

Notes: Peaks selected as local maxima of the $h = 1$ MUI at least 18 months apart, restricted to 1996 onward to exclude the initial estimation window. Associated events reflect the contemporaneous economic or political context and are not a claim that the named event caused the measured rise in uncertainty.

Figure 2 decomposes each CAPRD country's aggregate uncertainty into the share attributable to each of the eight underlying data categories over time. The decomposition is informative about structural change within countries independently of the cross-country connectedness question. Guatemala's uncertainty composition, for instance, shifts from a public-sector- and banking-dominated structure in the 1990s to an external-accounts-dominated structure from the mid-2000s onward, a pattern consistent with its growing integration into global trade and remittance flows. Panama's composition is dominated by public-sector uncertainty until approximately 2010, after which banking and interest-rate uncertainty take a much larger role, consistent with the deepening of its position as a regional financial and logistics hub. These within-country compositional shifts are not the object of the connectedness analysis that follows, but they are a reminder that each country's MUI has a recognisable economic anatomy rather than being a methodologically arbitrary summary statistic.

The term structure of uncertainty is itself worth illustrating before moving to the connectedness estimates, since the three horizons used throughout the paper, $h = 1$, 3, and 12 months, are not simply three independent snapshots of the same object. Figure 3 plots Costa Rica's MUI at all three horizons on a common scale. Two patterns recur across all seven CAPRD countries, not only Costa Rica. Longer-horizon uncertainty sits at a persistently higher level than short-horizon uncertainty, since a forecast twelve months ahead is mechanically harder to pin down than one month ahead, and the gap between the three horizons narrows during acute stress episodes and widens again as calm returns, so that the one-month, three-month, and twelve-month series briefly converge around 2008 to 2009 and again around 2020 before separating once more. This convergence during stress and separation during calm is one of the reasons the paper reports all three horizons throughout rather than treating $h = 1$ as sufficient on its own.

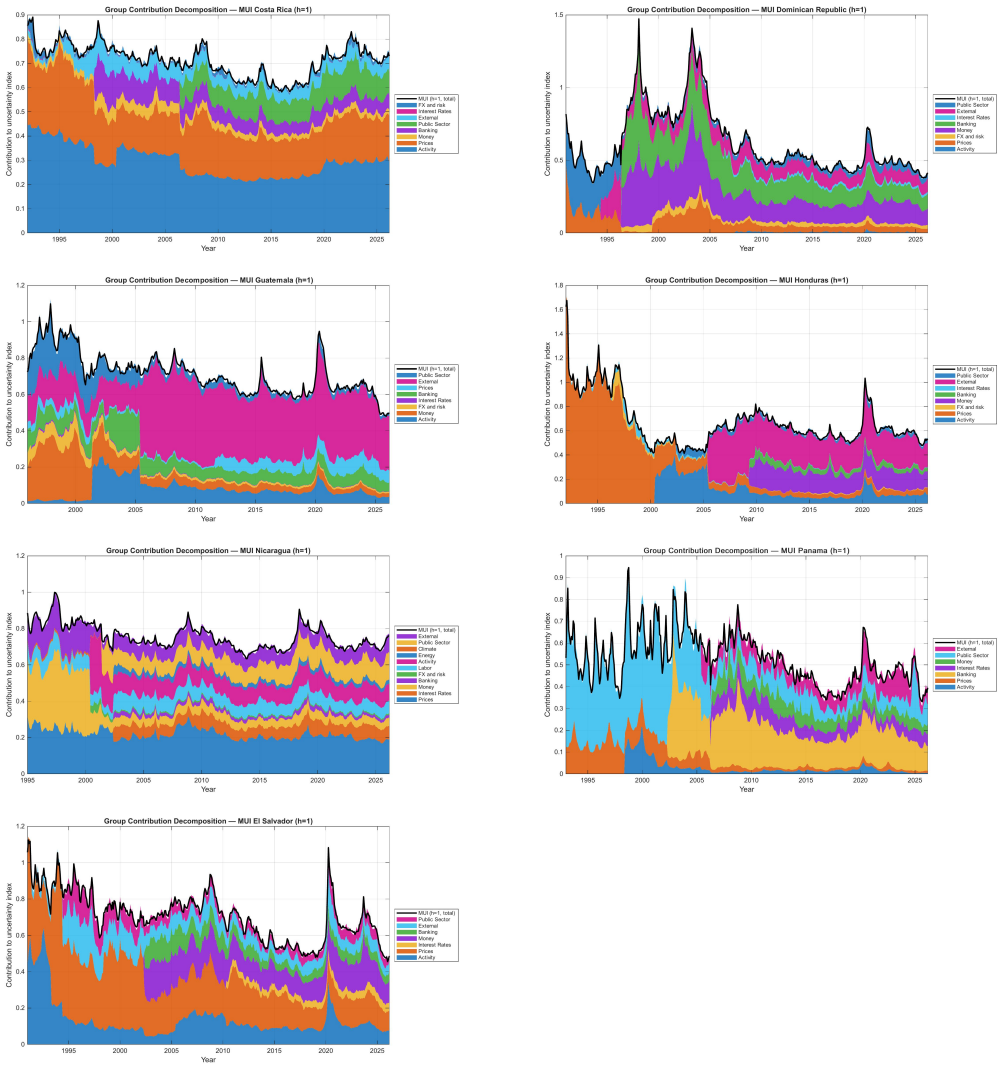


Figure 2: Category Contribution to Macroeconomic Uncertainty, by Country
Absolute contribution of each data block (Activity, Prices, Money, Banking, Public Sector, External, Interest Rates, FX and Risk, plus a small Labour, Climate, and Energy block for Nicaragua) to the level of $h = 1$-month MUI (black line), full available history through 2025:12. Source: own calculations.

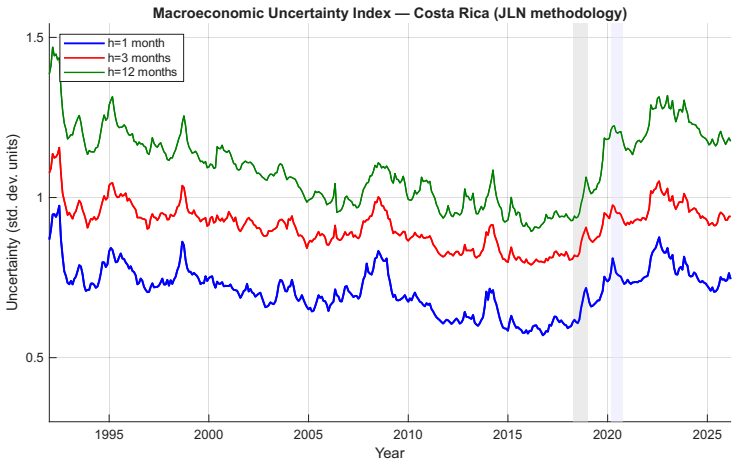


Figure 3: Macroeconomic Uncertainty Index Term Structure, Costa Rica
$h = 1$, $h = 3$, and $h = 12$ month MUI on a common scale, illustrating the narrowing of the term structure during stress episodes (shaded). Analogous patterns hold for the other six CAPRD countries. Source: own calculations.

4.2 Do the Factors Actually Capture Common Variation?

A construction of this kind is only as credible as the factors it rests on, and it is worth asking directly whether the small number of common macro and volatility factors extracted from each country's panel actually explain a meaningful share of what happens in the individual series that feed them, or whether the MUI is, in effect, summarising mostly noise. Following the diagnostic reported by Jurado et al. (2015) themselves, we regress each series in every country's panel on the estimated common macro factors $\hat{f}_t$ and separately on the estimated common volatility factors $\hat{g}_t$, and report the resulting R^2, averaged across all series in the panel and weighted by the number of series in each category. Table 2 summarises the result for all seven countries.

The common factors are far from a formality. Across the panel-wide average, the macro factors $\hat{f}_t$ explain between 26 % of cross-sectional variation in Nicaragua's series and 65 % in Honduras's, and the volatility factors $\hat{g}_t$, which are what ultimately feed the MUI itself, explain more still, between 28 % in Nicaragua and 71 % in Honduras. In every one of the seven countries the volatility-factor R^2 exceeds the macro-factor R^2, consistent with the JLN logic that uncertainty, defined as the conditional volatility of the unforecastable component, is if anything more strongly common across series than the levels or growth rates of the series themselves. Honduras, the Dominican Republic, and Panama, the three countries whose panels are most concentrated in a small number of categories, particularly External accounts and Interest Rates for Honduras and Panama, and Banking, Money, and Interest Rates for the Dominican Republic, show the highest overall R^2, while Nicaragua and Guatemala, whose panels are the most categorically diverse, including the Labour, Climate, and Energy blocks

unique to Nicaragua's data landscape, show the lowest. This is the expected pattern for a diffusion-index model, a panel dominated by a few closely related categories is mechanically easier for a handful of common factors to summarise than a panel spread thinly across many loosely related ones, and it is a useful piece of context for reading the category decompositions in Figure 2, where Nicaragua's and Guatemala's uncertainty is visibly distributed across a wider range of categories than Honduras's or the Dominican Republic's.

Table 2: Cross-Sectional Average R^2 of Common Factors, by Country

Country	Series in panel	Avg. R^2, macro factors $\hat{f}_t$	Avg. R^2, volatility factors $\hat{g}_t$
Costa Rica	119	0.286	0.338
Dominican Rep.	107	0.443	0.481
Guatemala	141	0.269	0.534
Honduras	114	0.645	0.707
Nicaragua	124	0.260	0.276
Panama	58	0.519	0.549
El Salvador	126	0.376	0.523

Each series' R^2 is from a regression of that series on the five estimated common macro factors ($\hat{f}_t$) or, separately, the three estimated common volatility factors ($\hat{g}_t$) used to build the country's MUI, following Jurado et al. (2015). Averages are weighted by the number of series in each of the eight to eleven data categories listed in Table 9 so that categories with more series do not mechanically dominate categories with few. Source: own calculations.

This diagnostic does not by itself validate any particular economic interpretation of the resulting MUI series. It validates the narrower and more basic claim that the factor extraction step is doing real work, that a handful of common factors meaningfully summarise dozens to well over a hundred country-specific series rather than compressing essentially unrelated data into an arbitrary index. Combined with the descriptive statistics and unit-root evidence in Section 5.1, it completes the case that the eight MUI series entering the connectedness analysis in Section 5.3 are measuring something real and common within each country's economy, before the paper turns to asking whether that measured uncertainty is also common *across* countries.

5 Results

The results proceed in three tiers, mirroring the two-stage empirical strategy of Section 3. Section 5.1 characterises the eight MUI series themselves, their distributional properties and their within-country variance structure, because these properties motivate the choice of quantile over mean-based inference in the network step. Section 5.3 turns to the QVAR connectedness network, the tail-amplification result, the static and dynamic network architecture, and the horizon dimension. Section 5.4 subjects the network to two verification exercises that speak to sampling uncertainty and to common-factor contamination.

5.1 Tier 1: The MUI Series and Their Within-Country Structure

5.1.1 Pre-estimation diagnostics

The descriptive statistics in Table 3 reveal a consistent pattern across all eight normalised MUI series. Seven of eight display significant excess kurtosis and Jarque-Bera statistics that decisively reject normality at $h = 1$; only Costa Rica cannot reject normality at conventional levels, with a Jarque-Bera p-value of 0.073.[3] This is not a technical inconvenience. It is the empirical signature of the phenomenon under study. Uncertainty is calm most of the time and explosive occasionally, and a framework that characterises only the conditional mean will, by construction, understate what happens when all eight economies are simultaneously in a high-uncertainty regime. That is the inference gap the QVAR is designed to fill.

The moments are also informative in their own right. Nicaragua carries the highest mean MUI among the eight (0.753 at $h = 1$), Honduras and the Dominican Republic show the region's highest standard deviations (0.176 and 0.228), and the Dominican Republic shows by far the most extreme positive skewness (1.27), consistent with its history of sharply concentrated uncertainty spikes, namely the 1998 and 2003 to 2004 episodes visible in Figure 1, rather than a broad distribution of moderately elevated readings. Costa Rica and Nicaragua show the region's lowest standard deviations (0.067 and 0.074), a finding that anticipates one of the paper's central results. Low mean-variance volatility, as the tail connectedness results below will show, does not imply low tail-networked exposure.

The unit root battery in Table 4 shows that the ADF test rejects the null of a unit root at the 5 % level in four of eight cases at $h = 1$ (Nicaragua, Panama, El Salvador,

[3] Honduras ($JB = 500$, $p < 0.001$) and the United States ($JB = 721$, $p < 0.001$) display the largest excess kurtosis, consistent with the concentration of large-uncertainty episodes around a small number of extreme events, as visible in the labelled peaks in Figure 1.

Table 3: Descriptive Statistics — Macroeconomic Uncertainty Index ($h = 1$ month)

Country	N	Mean	Med.	SD	Min	$Q_{.05}$	$Q_{.95}$	Max	JB	LB(12)
Costa Rica	368	0.703	0.707	0.067	0.570	0.592	0.815	0.876	5.2	2836***
Dominican Rep.	368	0.641	0.538	0.228	0.379	0.418	1.131	1.473	113***	3433***
Guatemala	368	0.714	0.687	0.117	0.533	0.597	0.976	1.090	89***	3311***
Honduras	368	0.632	0.564	0.176	0.479	0.496	1.061	2.116	500***	3301***
Nicaragua	368	0.753	0.737	0.074	0.611	0.658	0.885	1.020	50***	2680***
Panama	368	0.537	0.513	0.114	0.303	0.394	0.733	0.975	21***	2006***
El Salvador	368	0.685	0.684	0.118	0.478	0.501	0.888	1.223	30***	1747***
United States	368	0.658	0.622	0.120	0.527	0.545	0.893	1.239	721***	2253***

Sample: 1995:05 to 2025:12 ($T = 368$). MUI at $h = 1$ month, normalised cross-sectional average (Eq. 3).
JB = Jarque-Bera normality test statistic. LB(12) = Ljung-Box autocorrelation test at 12 lags.
*** $p < 0.01$; ** $p < 0.05$; * $p < 0.10$.

and the United States), while KPSS rejects stationarity for all eight at conventional levels. This combination is consistent with a highly persistent, near unit-root process for several series, a feature the literature has documented for bounded volatility series estimated from moderate-length panels (Ludvigson et al., 2021; Cascaldi-Garcia et al., 2023). This is reported for completeness. The QVAR does not require mean reversion or cointegration, since its identification relies on quantile-specific predictability rather than the long-run level of the series (Chatziantoniou et al., 2021).

Table 4: Unit Root Tests, MUI ($h = 1$ month)

Country	ADF	5 % c.v.	Reject H_0	KPSS	Order
Costa Rica	−2.78	−2.87	No	1.048	I(1)
Dominican Rep.	−1.70	−2.87	No	4.208	I(1)
Guatemala	−1.78	−2.87	No	4.836	I(1)
Honduras	−2.38	−2.87	No	3.364	I(1)
Nicaragua	−3.22	−2.87	Yes	2.773	Mixed
Panama	−4.51	−2.87	Yes	1.105	Mixed
El Salvador	−3.93	−2.87	Yes	1.715	Mixed
United States	−4.60	−2.87	Yes	0.630	Mixed

ADF: Augmented Dickey-Fuller test, H_0 is unit root, drift model. KPSS: H_0 is stationarity, 5 % critical value 0.463. All eight series reject the KPSS null, so the column reports the statistic itself alongside the resulting order classification.
Mixed indicates the ADF and KPSS tests point in different directions, a pattern common to highly persistent bounded volatility processes.

5.1.2 Within-country variance structure

Before asking how uncertainty moves between countries, it is worth asking what drives it within each country, since the answer bears on how the network results in Section 5.3 should be read. Figure 2 shows that the category composition of uncertainty is neither

stable across countries nor stable over time within a given country. The external-accounts share of uncertainty rises materially after 2005 in Guatemala and Honduras, the two CAPRD economies with the largest remittance-to-GDP ratios in the sample, a pattern consistent with growing exposure of domestic uncertainty to conditions in the migrant-sending US labour market rather than to purely domestic developments. Panama's banking- and interest-rate-uncertainty share rises sharply after 2010, tracking the deepening of its role as the region's dollarised financial centre. Price uncertainty is the single largest category almost everywhere in the sample except during country-specific institutional episodes that appear as temporary compositional breaks, for instance Guatemala's early-2000s public-sector-dominated years and Panama's pre-2010 public-sector dominance. None of this decomposition identifies a causal driver of any country's MUI. It documents which reduced-form data blocks the JLN factor procedure attributes the unforecastable variance to, country by country and period by period, and it is offered as context for interpreting the connectedness results that follow.

5.2 Tier 1.5: Country-Level Real Effects of Uncertainty

Before turning to the cross-country connectedness network, it is worth asking a narrower and more familiar question directly: within a single CAPRD economy, does a rise in that country's own MUI predict a subsequent slowdown in its own real activity, and if so, does that prediction hold uniformly across the growth distribution or specifically in its downside tail? Answering this requires two complementary country-by-country exercises that do not depend on the cross-country QVAR machinery of Section 5.3: a recursive VAR tracing the dynamic response of each country's own macro-financial variables to a domestic uncertainty shock, and a set of quantile regressions asking whether that predictive relationship is concentrated in particular quantiles of year-on-year activity growth.

5.2.1 Recursive VAR evidence

For each of the seven CAPRD economies we use a country-specific, Cholesky-identified recursive VAR estimated in levels or growth rates as appropriate to each series, with the country's own MUI (ordered first, consistent with the standard assumption that domestic uncertainty is not affected contemporaneously by the other variables in the system) and five or six macro-financial variables tailored to each country's data landscape and monetary regime. Estimation uses six lags, a 36-month impulse-response horizon, and a bootstrap confidence band at approximately the 90 % level. The variable set is not identical across countries because the monetary regime is not identical across countries. Costa Rica, the Dominican Republic, Guatemala, and Honduras retain independent currencies and therefore include an exchange-rate variable; Panama and El Salvador

are fully dollarised and have no exchange rate to include, so their systems instead carry Exports (Panama) or Remittances (El Salvador) as the additional external variable; and Nicaragua's system is the only one to include Employment growth alongside Activity growth, giving it seven variables in total rather than six.

Figure 4 plots the response of Costa Rica's system to a one-standard-deviation shock to its own MUI. Activity growth falls sharply on impact, oscillates through a damped cycle over the following eight months, and returns to baseline by roughly month 15; credit growth follows a similar damped-oscillation pattern before turning mildly negative at horizons beyond ten months; the lending rate falls by up to 12 percentage points at its trough around month 6 before reversing sign and rising modestly through month 20; and both inflation and FX growth show the same short-lived overshoot-and-reversion pattern within the first six months. This is the signature of a demand-side uncertainty shock working through a conventional monetary and credit channel, activity and credit fall, borrowing costs initially ease as monetary policy responds, and the system normalises within one to two years.

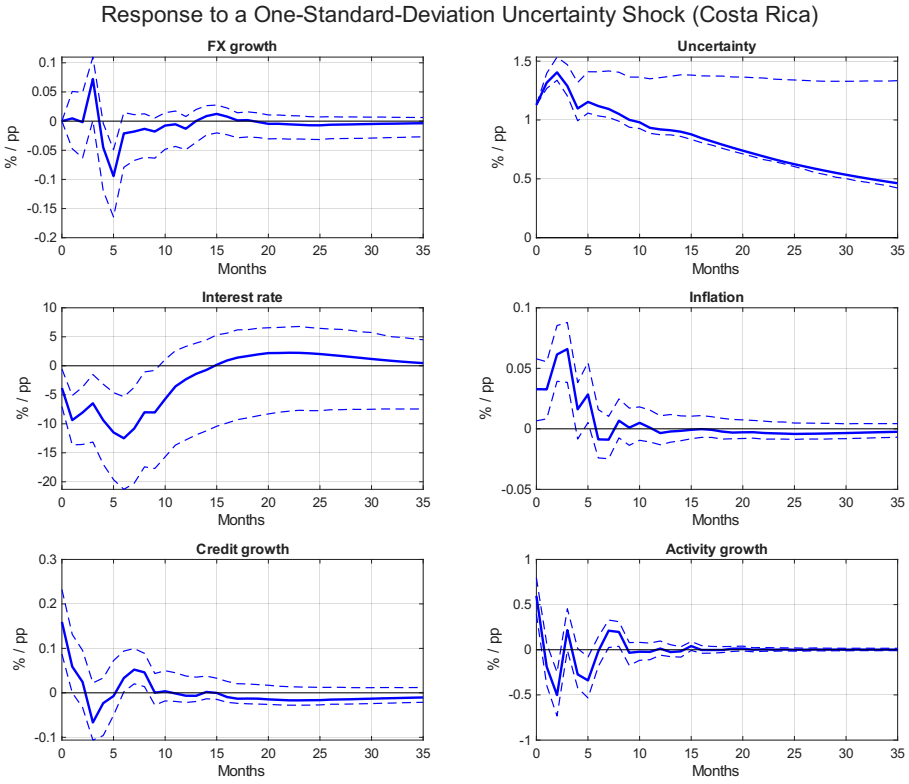


Figure 4: Response to a One-Standard-Deviation Uncertainty Shock, Costa Rica
Recursive (Cholesky) VAR, MUI ordered first, 36-month horizon. Solid line: point estimate. Dashed lines: bootstrap confidence band. Source: own calculations.

Figure 5 repeats the exercise for Nicaragua, whose network role at long horizons is the paper's central horizon-sensitive finding in Section 5.3. Nicaragua's own system

responds to a domestic uncertainty shock with a sharp initial contraction in activity growth of similar magnitude to Costa Rica's, but two features distinguish it. First, the interest rate response is the opposite sign, Nicaragua's interest rate *rises* by six to eight percentage points at its peak around month 8, rather than falling as in Costa Rica, a pattern more consistent with a risk-premium or liquidity-scarcity response than with a conventional monetary easing. Second, employment growth, a variable unique to the Nicaraguan system, falls by 15 to 20 percentage points on impact and takes roughly 15 months to recover, and credit growth is the most persistently negative of any variable in any of the seven country systems, still 8 to 10 percentage points below baseline after two years. Nicaragua's domestic uncertainty shock therefore appears to leave a materially deeper and more persistent mark on credit and employment than the shocks estimated for the other six economies, consistent with the idea that Nicaragua's uncertainty is not merely a regional transmitter in the cross-country network documented in Section 5.3 but also carries unusually large real domestic consequences of its own.

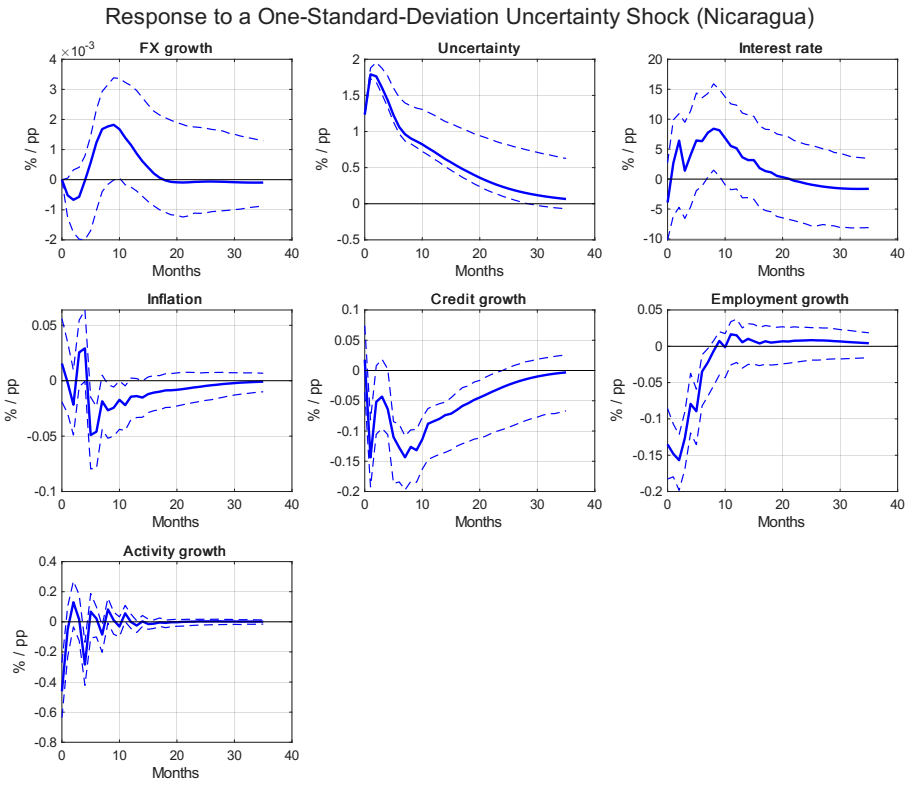


Figure 5: Response to a One-Standard-Deviation Uncertainty Shock, Nicaragua
Same conventions as Figure 4. The Nicaraguan system additionally includes Employment growth, not estimated for the other six countries.

The remaining five country systems, reported in full in Figures 16 through 20 in the Appendix, add further heterogeneity rather than repeating a single template. Guatemala's activity growth response is the only one in the sample to *overshoot into*

positive territory, falling initially, then rising to roughly +0.15 percentage points around month 5 before decaying to zero, a pattern that recurs, with somewhat different timing, in El Salvador's activity response. Honduras's response is a closer match to Costa Rica's, a sharp initial contraction followed by a damped oscillation and convergence within about 15 months. Panama's system, the only one to include Exports rather than an exchange rate, shows the largest initial swing of any country, activity falling to nearly −2 percentage points and exports to nearly −2 percentage points on impact, before both rebound sharply within the first six months, consistent with the idea that a highly trade- and logistics-dependent, fully dollarised economy transmits uncertainty shocks through trade volumes rather than through the exchange rate or an independent policy rate. El Salvador's system, the only one to include Remittances, shows a similarly sharp initial contraction in remittance growth, falling to −2 to −3 percentage points on impact, before rebounding to a positive overshoot of roughly +1.5 points by month 3 and then decaying, a pattern that plausibly reflects a short-run precautionary or timing response by the Salvadoran diaspora rather than any change in the fundamental remittance relationship. The Dominican Republic stands out for the sheer persistence of its own MUI response to its own shock, still elevated by roughly 0.8 index points at month 35, more than double the persistence seen in any other CAPRD country, and its activity response is the deepest on impact of the six countries with an activity panel labelled "Activity" rather than "Activity growth," falling to beyond −1.3 percentage points before a damped recovery.

These country-level VARs are estimated one economy at a time and are silent on cross-border transmission. Their purpose is narrower and more foundational than the connectedness network of Section 5.3, to establish that each country's own MUI is not merely a statistical construct but predicts a materially worse activity and credit path in that same country, at the conditional mean, and that the channel through which this plays out, the exchange rate in the four non-dollarised economies, exports in Panama, remittances in El Salvador, employment in Nicaragua, differs in ways that track each country's actual economic structure. That finding is the necessary premise for asking, as Section 5.3 does, whether the cross-border transmission of these domestically consequential shocks itself changes shape under stress.

5.2.2 Quantile regression evidence: where in the growth distribution does uncertainty bind?

The VAR evidence above describes the average dynamic response of activity growth to an uncertainty shock. It does not say whether that average response is driven by a broad, uniform shift in the growth distribution or by a concentrated effect on its worst outcomes, and it says nothing about whether the size of that effect is actually

comparable from one country to the next, since MUI and activity growth are measured on entirely different scales in each of the seven economies. To answer both questions at once we standardise every variable, subtracting its country-specific mean and dividing by its country-specific standard deviation, before estimating a quantile regression of each country's own year-on-year activity growth on its contemporaneous MUI, its own first lag of activity growth, and year-on-year credit growth as a financial-conditions control,

$$\tilde{y}_{i,t} \;=\; \alpha_\tau \;+\; \beta_\tau \,\widetilde{\mathrm{MUI}}_{i,t} \;+\; \gamma_\tau \,\tilde{y}_{i,t-1} \;+\; \delta_\tau \,\widetilde{\mathrm{Credit}}_{i,t} \;+\; \varepsilon_{i,t}(\tau), \qquad \tau \in \{0.05, \ldots, 0.95\}, \tag{17}$$

where a tilde denotes the standardised (zero-mean, unit-variance) version of each series, estimated separately at seven quantiles ($\tau = 0.05, 0.10, 0.25, 0.50, 0.75, 0.90, 0.95$) using the Koenker and Bassett (1978b) quantile-regression estimator, with credit growth serving as the readily available proxy for domestic financial conditions given that a comparable interest-rate spread series is not uniformly available across all seven countries at monthly frequency. Standardising before estimation means β_τ is no longer denominated in percentage points of activity growth per index point of MUI, a unit that differs in scale from country to country, but in standard deviations of activity growth per standard deviation of MUI, a unit that is directly comparable across the seven economies regardless of how volatile each country's own growth or uncertainty series happens to be.

Table 5 reports the standardised coefficient on MUI at the lower tail, the median, and the upper tail of each country's own activity-growth distribution. The pattern is strikingly consistent across five of the seven economies. In Costa Rica, the Dominican Republic, Honduras, Nicaragua, and El Salvador, the MUI coefficient is substantially negative and statistically significant at the 5th percentile of activity growth, shrinks toward zero by the median, and is statistically indistinguishable from zero, or in Costa Rica's case significantly positive, at the 95th percentile. Honduras and the Dominican Republic show the sharpest version of this pattern, a one-standard-deviation rise in MUI is associated with activity growth that is 0.56 and 0.52 standard deviations lower, respectively, at the 5th percentile ($p < 0.001$ in both cases), against a statistically insignificant effect at the median in Honduras and only a modest, marginally significant effect in the Dominican Republic. Because every coefficient in Table 5 is now measured in the same standard-deviation units, the cross-country ranking is informative in a way the raw-scale coefficients could not be, Honduras and El Salvador show the largest standardised lower-tail exposure to their own uncertainty (-0.560 and -0.532 at $\tau = 0.05$), followed by the Dominican Republic and Nicaragua (-0.520 and -0.356), with Costa Rica somewhat more moderate (-0.202). Put in the language this paper commits to throughout, our quantile-regression estimates show that a one-standard-deviation rise in domestic

uncertainty is associated with activity growth between one-fifth and over one-half of a standard deviation lower at the bottom of the growth distribution, a materially larger effect than the same shock has on the centre of the distribution, for the majority of CAPRD economies in this sample. Guatemala and Panama do not fit this pattern. Guatemala's standardised MUI coefficient is small and not statistically significant at either tail, and Panama's coefficient is not statistically significant at any reported quantile, indicating that the downside-tail-amplification finding, while common and now directly comparable in magnitude across the five countries that exhibit it, is not universal across the CAPRD.

Table 5: Quantile Regression of Standardised Activity Growth on Standardised Own MUI, Selected Quantiles

Country	$\beta_{0.05}$ (MUI)	$\beta_{0.50}$ (MUI)	$\beta_{0.95}$ (MUI)	N
Costa Rica	-0.202^{**}	-0.017	$+0.213^{**}$	327
Dominican Rep.	-0.520^{***}	-0.086^{**}	$+0.032$	218
Guatemala	$+0.069$	-0.039	-0.096	362
Honduras	-0.560^{***}	-0.049	$+0.075$	195
Nicaragua	-0.356^{***}	-0.201^{***}	$+0.038$	278
Panama	$+0.009$	$+0.050$	-0.073	231
El Salvador	-0.532^{***}	-0.054	$+0.232^{*}$	278

Dependent variable: year-on-year growth of the country's principal monthly activity indicator, standardised to zero mean and unit variance within each country. Regressors, all standardised in the same way: contemporaneous MUI (own, $h = 1$), one-month lag of the dependent variable, and year-on-year credit growth (coefficient not reported; see Figure 6). Because every variable is standardised, β_τ is directly comparable across countries and reads as the change in activity growth, in standard-deviation units, associated with a one-standard-deviation change in MUI. Quantile regression, Koenker and Bassett (1978b) estimator.
$^{***}\,p < 0.01$; $^{**}\,p < 0.05$; $^{*}\,p < 0.10$.

Figure 6 plots the full standardised coefficient path across all seven estimated quantiles for each country, together with a 95 % confidence band, on a common vertical scale that is only meaningful because every coefficient has been placed in the same standard-deviation units. In the five countries for which Table 5 shows a significant lower-tail effect, the coefficient path is monotonically increasing in τ, moving from a large negative value at the lower quantiles through zero near the median to a near-zero or positive value at the upper quantiles. This shape, an upward-sloping quantile coefficient path that crosses zero near the centre of the distribution, is the same signature that Chatziantoniou et al. (2021) document for cross-country tail-connectedness and that this paper's own QVAR results document for the cross-border network in Section 5.3.1. At the single-country level, exactly as at the cross-country network level, the consequences of uncertainty are concentrated in the tail rather than spread evenly across the distribution, and

standardisation now lets that statement be made in a common currency across all seven economies rather than country by country.

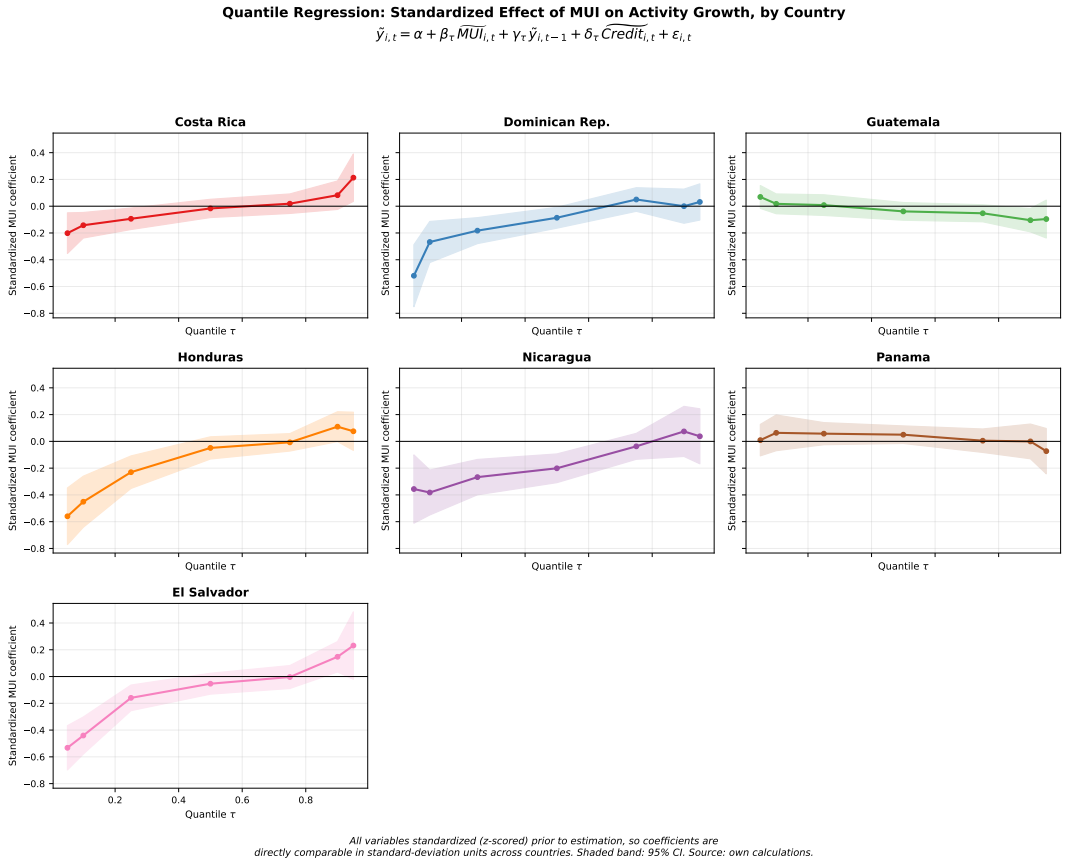


Figure 6: Quantile Regression Coefficient on Standardised MUI, Standardised Year-on-Year Activity Growth, by Country

Coefficient β_τ from Eq. 17 at seven quantiles ($\tau = 0.05, \ldots, 0.95$), all variables standardised (zero mean, unit variance) within each country prior to estimation, so the vertical axis is directly comparable across panels. Shaded band: 95 % confidence interval from quantile-regression standard errors. Source: own calculations.

As with the cross-country QVAR estimates, these country-level quantile regressions are reduced-form predictive relationships for this sample and this specification. They document that domestic uncertainty predicts materially worse downside activity outcomes in most, though not all, CAPRD economies, that this predictive relationship strengthens toward the lower tail of the growth distribution, and, now that the coefficients are standardised, that Honduras and El Salvador carry the largest such exposure in the region while Guatemala and Panama carry essentially none. They do not identify why Guatemala and Panama depart from the regional pattern, a question that, like the country-specific departures documented in Section 5.3, is left open for future work using higher-frequency or more disaggregated domestic data.

5.3 Tier 2: QVAR Connectedness, The Network Architecture

5.3.1 The central result: tail amplification

The headline finding of this paper is that the CAPRD uncertainty network is not merely connected at the mean. It amplifies at the upper tail. Table 6 makes this visible in a single row. At $h = 1$ and the median ($\tau = 0.50$), the TCI is 26.5 %. In a typical month, roughly a quarter of every dollar of a country's forecast error variance in its own MUI traces to shocks originating elsewhere in the network, a magnitude consistent with prior estimates of uncertainty connectedness across small open economies (Gabauer and Gupta, 2018; Antonakakis et al., 2018). At the upper tail ($\tau = 0.95$), the months in which all eight economies are simultaneously experiencing high uncertainty, the TCI rises to 94.0 %, a ratio of 3.5 relative to the median. In those months the region is almost entirely systemic. The amplification is present at every horizon considered. At $h = 3$ the ratio is 4.5 (91.0 % against 20.2 %), and at $h = 12$ it is 4.2 (71.2 % against 17.1 %). The $h = 12$ upper-tail TCI is somewhat lower than at $h = 1$ and $h = 3$, which indicates that the amplification, while present at every horizon, is strongest at short and medium horizons and moderates somewhat at the twelve-month horizon rather than growing without bound.

Table 6: Total Connectedness Index (TCI), Full-Sample QVAR Estimates

	Lower tail ($\tau = 0.05$)	Median ($\tau = 0.50$)	Upper tail ($\tau = 0.95$)
$h = 1$ month	84.7 %	26.5 %	94.0 %
$h = 3$ months	82.7 %	20.2 %	91.0 %
$h = 12$ months	75.0 %	17.1 %	71.2 %

QVAR($p = 2$), forecast horizon nfore = 12, 48-month rolling window for the dynamic estimates, corrected GFEVD for the static estimates reported here. Sample: 1995:05 to 2025:12 ($T = 368$).
The TCI measures the fraction of total forecast error variance accounted for by cross-country uncertainty shocks rather than own shocks.
The lower-tail TCI is also elevated. The economically relevant asymmetry is the median-to-upper-tail ratio, discussed below, rather than the level of the lower tail on its own.

This result deserves careful interpretation. The QVAR estimates do not identify a causal mechanism through which high uncertainty in one economy propagates to another. They identify that the conditional quantile of the system exhibits strong predictive cross-economy linkages at the upper tail (Diebold and Yilmaz, 2014). What the data reveal is that the structure of uncertainty transmission changes substantially with the prevailing regime. At the median, each economy's MUI trajectory is largely determined by its own domestic history. At the ninety-fifth percentile, a regime that occurs when the kind of first-moment shocks documented by Bloom (2009) and Ludvigson et al. (2021) affect multiple economies simultaneously, the network transmits nearly the entirety of each country's forecast error variance across borders. Put in the language this paper

commits to throughout, our QVAR estimates show that the region's uncertainty network expands from transmitting roughly a quarter of forecast-error variance across borders at the median to transmitting ninety-four percent at the upper tail at a one-month horizon, a finding about the shape of the estimated network under this sample and this method, not a statement about any underlying transmission law.

The lower-tail TCI ($\tau = 0.05$) is also high, at 84.7 % at $h = 1$, though for a different statistical reason. In the GFEVD framework, extreme low-uncertainty regimes are also predictably networked, because the observations driving the quantile regression are themselves a small, selected set whose co-movement is systematic (Chatziantoniou et al., 2021). The important asymmetry, accordingly, is not between the upper and lower tails, but between the tails and the median.

5.3.2 Who transmits and who receives

The full-sample static connectedness tables (Tables 7 and 8) show that the direction of uncertainty transmission is not symmetric across the CAPRD and shifts between the median and the upper tail.

The United States as the dominant systemic transmitter. At the median, the United States transmits 34.0 percentage points more forecast error variance to other economies than it receives from them, and at the upper tail this net transmission position widens to +98.3 percentage points, the largest absolute NET value in the system at $h = 1$. In the GFEVD matrix at $\tau = 0.95$, US uncertainty explains between 6.1 % (Guatemala) and 26.8 % (Costa Rica) of every CAPRD country's forecast error variance, a range that in most cases exceeds the pairwise contribution any single CAPRD neighbour makes, consistent with the role of US monetary-policy expectations, global risk sentiment, and commodity-price shocks as dominant exogenous uncertainty drivers for small open economies (Biljanovska et al., 2021; Andres-Escayola et al., 2025).

Honduras as a persistent intra-regional transmitter. Honduras is the second-largest net transmitter at the upper tail, with NET = +18.1 percentage points at $\tau = 0.95$, $h = 1$, and it is also the largest net transmitter at the median (NET = +21.7). The GFEVD rows show Honduras contributing between 6.6 % and 22.5 % of forecast error variance to the other seven economies at the upper tail. One plausible reading, consistent with the documentation of political uncertainty and governance fragility in the region by Molina et al. (2023) and Diakonova et al. (2024), is that Honduras's elevated structural uncertainty, combining political instability, security crises, and climate exposure, makes its uncertainty regime informative about the regional tail. When Honduras's MUI sits at its ninety-fifth percentile, that reading predicts high uncertainty throughout the region.

This is a predictive rather than causal relationship, and whether it reflects genuine spillovers through trade and financial linkages or co-movement driven by common external shocks that reach Honduras first is a question beyond what the QVAR can identify on its own.

Panama and the Dominican Republic as the most exposed receivers at short horizons. At $h = 1$, $\tau = 0.95$, Panama carries the largest negative net position in the system (NET $= -46.6$), followed by the Dominican Republic (NET $= -29.9$) and Nicaragua (NET $= -25.2$). Costa Rica is also a net receiver at this specification (NET $= -26.2$), a role it retains at every horizon and quantile combination examined in this paper except one, discussed below. Panama's position as a receiver despite its role as the regional financial hub is consistent with the hypothesis that financial-sector uncertainty is imported rather than domestically generated during stress episodes. The openness that makes Panama's financial system a regional intermediary also makes it a conduit for imported uncertainty. The Dominican Republic's receiver status is consistent with its structural profile as the most tourism- and US-exposed economy among the eight, with a financial sector whose history of crisis episodes, visible in its 1998 and 2003 to 2004 MUI peaks in Figure 1, creates vulnerability to external uncertainty shocks (Diakonova et al., 2025).

The median reveals a more dispersed architecture. At $\tau = 0.50$, Honduras and the United States are the two clear net transmitters, Costa Rica and Nicaragua are the largest net receivers, and the median network is less concentrated around a single dominant hub than the upper-tail network. This is not a sign that one architecture is more representative than the other. The two characterise different moments of the uncertainty distribution and correspond to genuinely different economic states, the typical month and the month in which the transmission matters most.

Table 7: Static Connectedness Table, $h = 1$ month, Median ($\tau = 0.50$)

From↓ / *To*→	CRI	DOM	GTM	HND	NIC	PAN	SLV	USA	FROM
CRI	72.54	5.02	0.04	4.20	0.43	2.43	0.83	14.51	27.46
Dominican Rep.	2.47	77.12	5.98	8.91	0.18	1.59	0.21	3.55	22.88
Guatemala	0.55	1.01	67.95	18.68	0.38	1.40	5.59	4.45	32.05
Honduras	0.45	0.35	8.68	75.47	1.85	1.99	6.47	4.73	24.53
Nicaragua	1.90	0.03	5.65	12.24	72.39	1.53	2.96	3.29	27.61
Panama	0.25	0.48	1.08	0.76	0.25	89.19	5.56	2.43	10.81
El Salvador	3.09	0.86	6.17	0.86	0.32	7.68	69.82	11.21	30.18
United States	2.22	0.10	0.64	0.61	3.63	1.05	1.89	89.86	10.14
TO	10.92	7.86	28.24	46.26	7.04	17.66	23.51	44.17	
NET	−16.54	−15.02	−3.81	+21.74	−20.56	+6.84	−6.67	+34.03	
TCI = 26.52 %									

Entry (i, j), row i, column j, is the percentage of row i's $H = 12$-step MSFE explained by shocks originating in column j. FROM is the row total received. TO is the column total transmitted. NET equals TO minus FROM.

Table 8: Static Connectedness Table, $h = 1$ month, Upper Tail ($\tau = 0.95$)

From↓ / To→	CRI	DOM	GTM	HND	NIC	PAN	SLV	USA	FROM
CRI	16.37	8.68	10.68	7.25	9.89	8.08	12.21	26.84	83.63
Dominican Rep.	8.72	10.95	13.36	20.43	8.58	7.22	16.20	14.53	89.05
Guatemala	3.74	2.38	11.75	8.43	2.69	1.46	9.03	60.52	88.25
Honduras	8.64	9.03	14.15	20.52	9.64	6.64	16.55	14.83	79.48
Nicaragua	5.86	12.79	16.27	22.20	14.33	6.10	11.45	11.00	85.67
Panama	9.62	13.00	13.91	18.05	11.48	11.29	14.48	8.16	88.71
El Salvador	9.48	7.29	13.88	15.20	9.68	5.74	16.43	22.30	83.57
United States	11.40	5.96	8.50	6.05	8.49	6.89	12.58	40.13	59.87
TO	57.47	59.13	90.76	97.61	60.44	42.13	92.51	158.18	
NET	−26.16	−29.91	+2.51	+18.13	−25.24	−46.58	+8.94	+98.31	
TCI = 94.03 %									

Same conventions as Table 7. At $\tau = 0.95$ every FROM value exceeds 79 %, indicating near-total systemic integration of the network during high-uncertainty episodes. Guatemala's own diagonal falls to 11.75 %, its lowest own-variance share of any specification, while the United States retains the highest own-variance share (40.13 %), consistent with the partial exogeneity of US uncertainty from a CAPRD perspective.

5.3.3 The network visualised

Figure 7 translates the static connectedness tables into directed network graphs, drawing an edge from country j to country i whenever the pairwise contribution exceeds a common global threshold, with node fill colour indicating net-transmitter (red) versus net-receiver (blue) status and node size scaled to |NET|. At the median (left panel) the graph is comparatively sparse, dominated by a handful of edges radiating from Honduras and the United States. At the upper tail (right panel) the graph is visibly denser, and the United States sits as the largest node with outflows toward every other economy in the system. Two features of the architecture deserve emphasis beyond the pairwise numbers already discussed. The hub-and-spoke reading is only partially correct. The United States generates outflows toward every other node at the upper tail, making it the clear hub, but the connections among CAPRD economies themselves are dense enough that the network is not star-shaped. Guatemala, Honduras, El Salvador, and the Dominican Republic exchange substantial pairwise shares among themselves in addition to receiving from the United States, and this density is itself a finding. Intra-CAPRD uncertainty transmission has independent predictive content at the upper tail beyond what a simple relay of US shocks would generate, consistent with the trade and financial integration documented by Urbina and Marenco (2024). Figures 8 and 9 repeat the same comparison at $h = 3$ and $h = 12$ months and are discussed together with the horizon dimension in Section 5.3.5.

A complementary chord-diagram representation of the same six specifications, showing the gross pairwise contribution between every pair of economies rather than only the edges that clear a threshold, is provided in Figures 13 through 15 in the Appendix for readers who want the full pairwise detail underlying Figures 7 through 9. Consistent

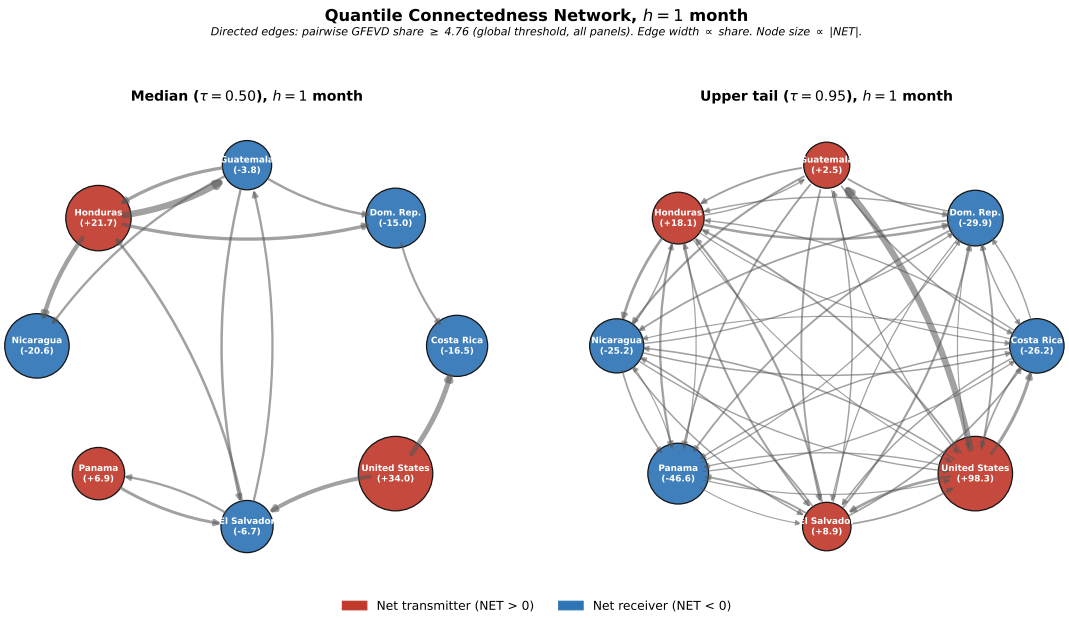


Figure 7: Quantile Connectedness Network, $h = 1$ Month

Left: median ($\tau = 0.50$). Right: upper tail ($\tau = 0.95$). Directed edges drawn for pairwise GFEVD shares at or above a common global threshold (the median of all pooled off-diagonal cells across the six panels used in this paper). Arrow direction: from transmitter to receiver. Node colour: red = net transmitter (NET > 0), blue = net receiver (NET < 0); node size scales with |NET|. Data: 1995:05 to 2025:12; QVAR($p = 2$), nfore = 12, corrected GFEVD. Source: own calculations.

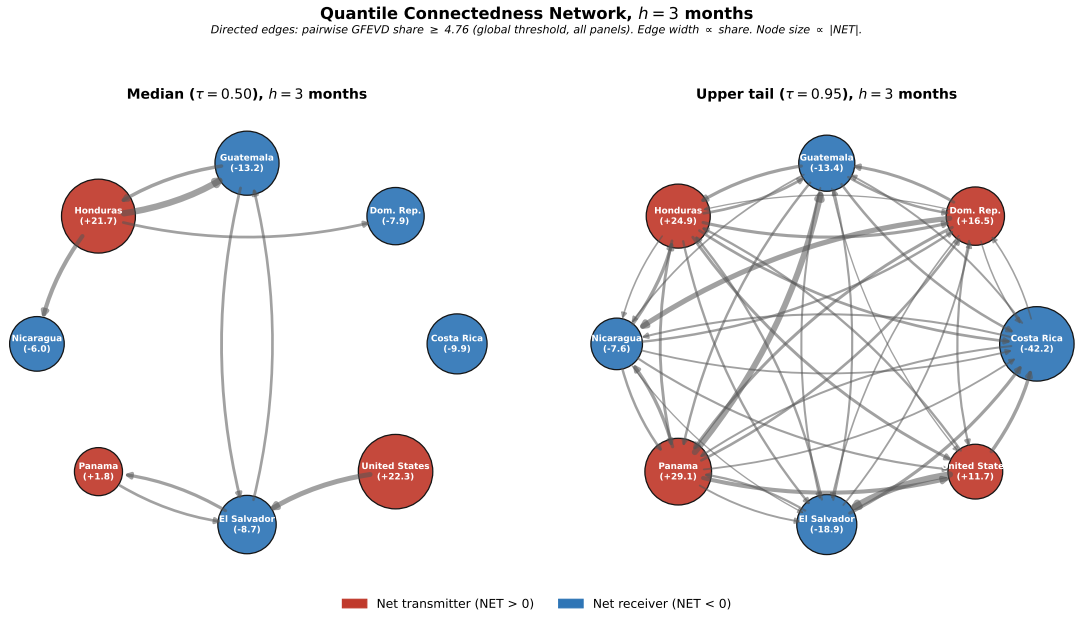


Figure 8: Quantile Connectedness Network, $h = 3$ Months

Same conventions as Figure 7.

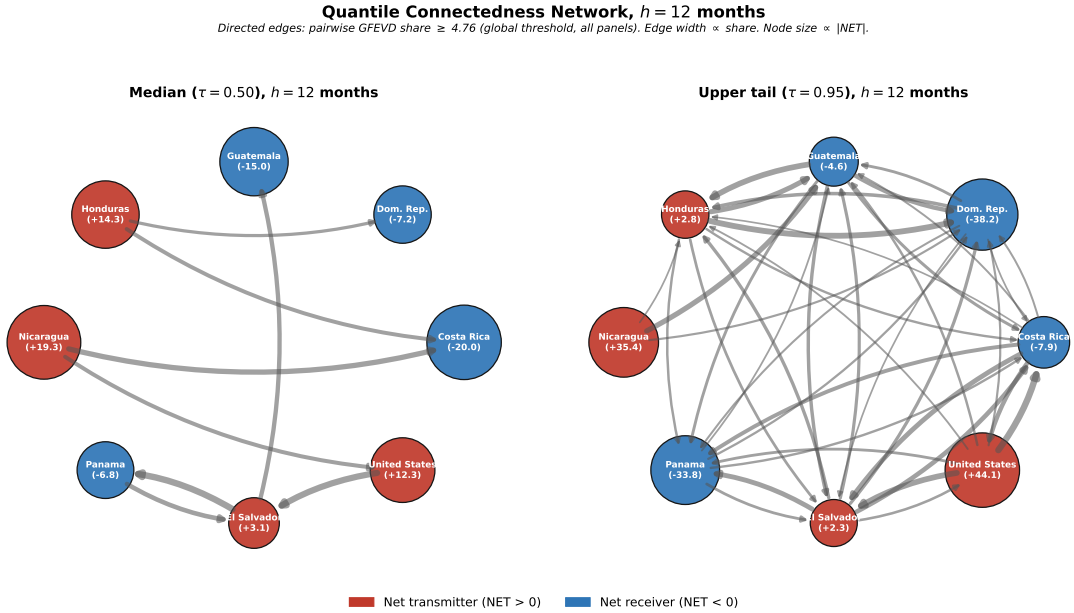


Figure 9: Quantile Connectedness Network, $h = 12$ Months
Same conventions as Figure 7.

with the network figures, no country's own-shock (diagonal) contribution is shown in the chord diagrams; every ribbon is a genuine cross-country pairwise flow.

5.3.4 Dynamic connectedness, how the network moves through time

The rolling-window estimates in Figure 10 show that the tail amplification documented in the full-sample TCI is not a fixed constant. Its intensity varies across the sample's stress episodes and across the twelve-month rolling window in ways that a single number cannot convey. At $h = 1$, the upper-tail TCI stays in a comparatively narrow band above 90 % for almost the entire sample, while the median TCI swings between roughly 60 % and 100 %, occasionally approaching the upper-tail level during periods of broad-based stress and falling well below it during calmer stretches of the 2000s and mid-2010s. This pattern repeats at $h = 3$ and $h = 12$, though the median series becomes noticeably more volatile at longer horizons, consistent with the term-structure narrowing illustrated for Costa Rica in Figure 3.

Figure 11 extends the net directional analysis across all nine horizon-quantile combinations using the full-sample static estimates. Three cross-cutting patterns emerge. The United States is a net transmitter in seven of the nine specifications and its transmitter role strengthens at the upper tail relative to the median at every horizon, confirming that US dominance becomes proportionally more pronounced precisely in the stress regimes where its impact on CAPRD economies is most consequential. Costa Rica is a net receiver in eight of the nine specifications, the sole exception being $h = 3$ at the median, where its net position is close to zero, so its receiver status is the most stable

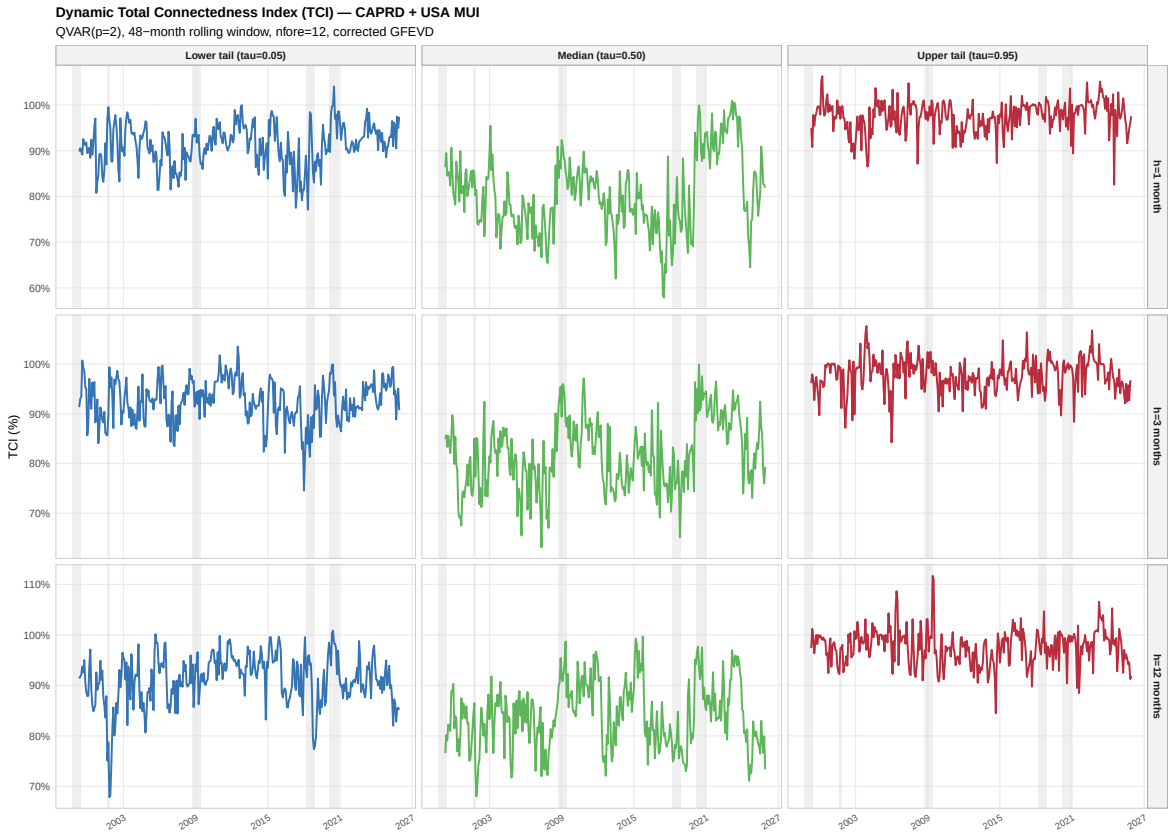


Figure 10: Dynamic Total Connectedness Index (TCI), 48-Month Rolling Window
Columns: quantile ($\tau = 0.05, 0.50, 0.95$). Rows: forecast horizon ($h = 1, 3, 12$ months). QVAR($p = 2$), nfore = 12, corrected GFEVD. Shaded bands mark the major stress episodes discussed in the text. Source: own calculations.

feature in the entire array rather than an artefact of any single specification. Nicaragua, by contrast, moves between roles depending on the horizon. It is a modest net receiver at $h = 1$ and a substantial net transmitter at $h = 12$, most strikingly at the upper tail, where NET $= +35.4$, the second-largest transmitter position in the entire array after the United States at the same horizon. This reversal, from receiver at short horizons to transmitter at the long horizon and upper tail, is the most horizon-sensitive finding in the paper and is examined further below.

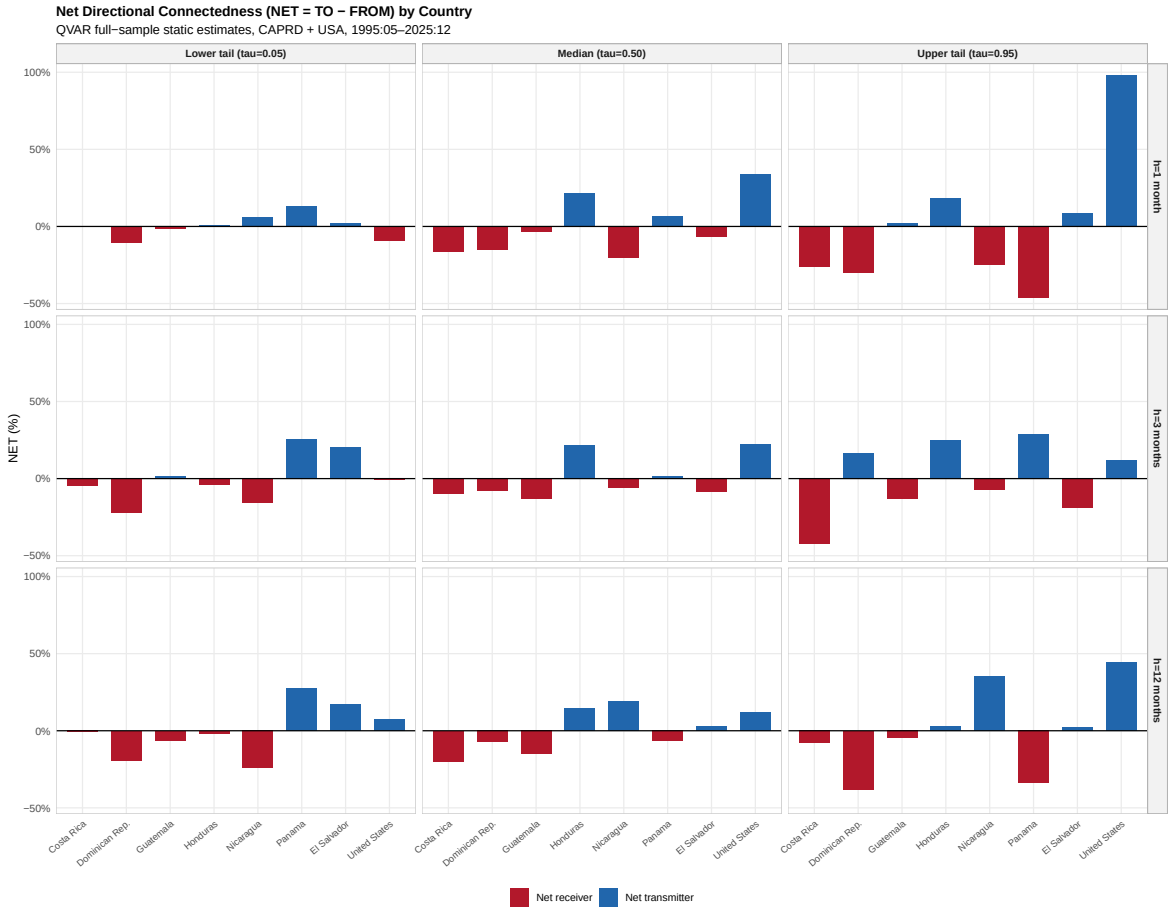


Figure 11: Net Directional Connectedness (NET = TO minus FROM), All Specifications
Blue bars indicate net transmitters, red bars net receivers. Columns: quantile. Rows: forecast horizon. QVAR($p = 2$), nfore = 12, corrected GFEVD, full sample. Source: own calculations.

Figure 12 plots the rolling-window NET for all eight economies at $h = 1$, disaggregated by country, with all three quantiles overlaid so the tail-versus-median distinction can be read within each panel. The United States upper-tail line sits above its median line for almost the entire sample, confirming that its dominance is a structural feature of the network rather than an artefact of any single stress episode, while its median line fluctuates between positive and negative across the thirty-year sample, indicating that transmitter dominance is specifically a tail phenomenon that a mean-based analysis would understate. Guatemala's upper-tail net position spikes sharply and repeatedly between 2015 and 2022, reaching levels above 400 % during several sub-windows, the

largest transient swings of any country in the sample, while its median position stays close to zero throughout, illustrating in the starkest terms available in this dataset how a mean-based connectedness analysis can miss an economically large, tail-specific transmission episode entirely. Nicaragua's dynamic pattern mirrors the static finding above. Its upper-tail net position is close to zero or negative for most of the sample before rising sharply from around 2015 and again after 2020, consistent with the emergence of a long-horizon transmitter role that the static $h = 12$ estimates capture as a full-sample average.

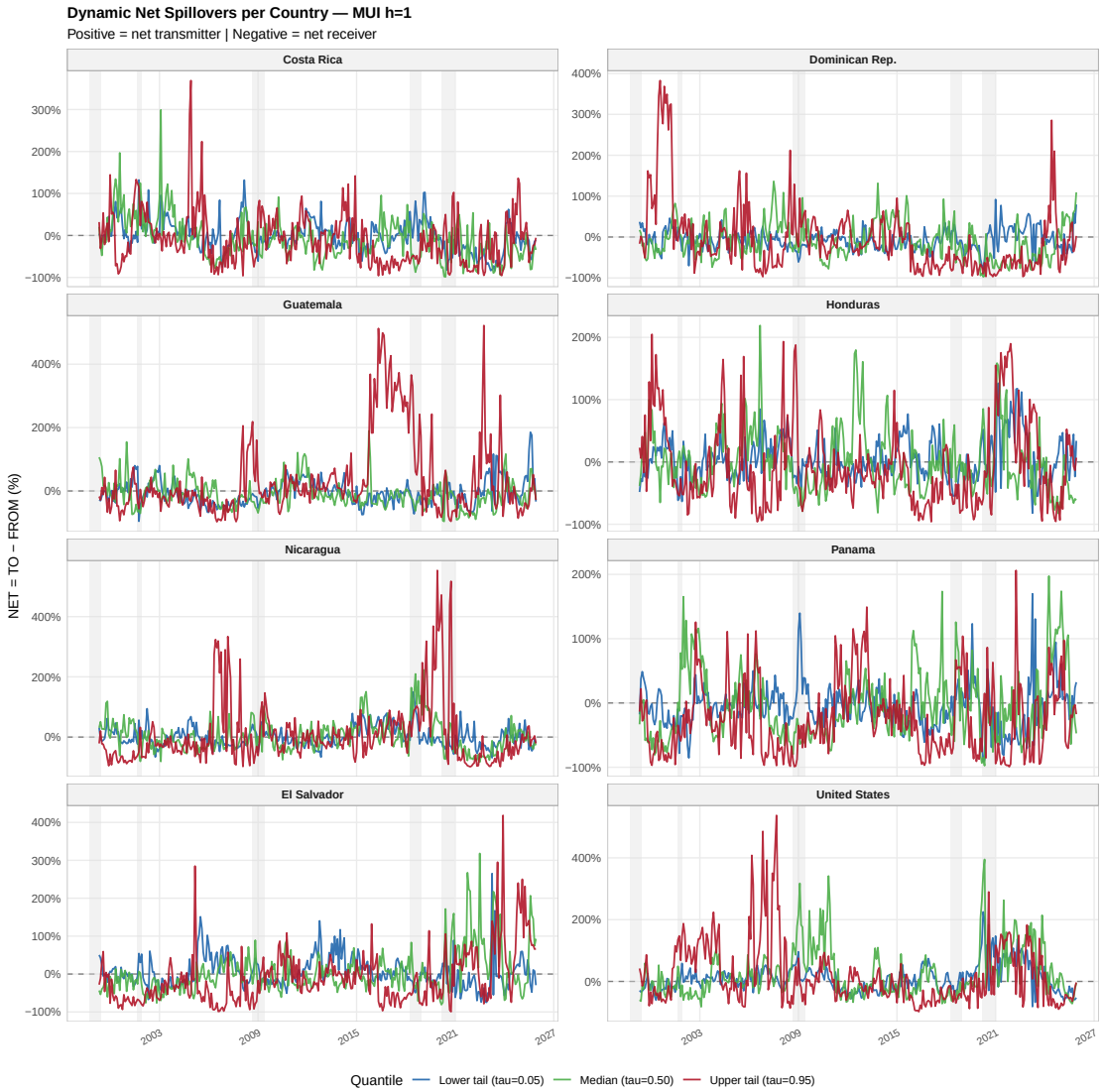


Figure 12: Dynamic Net Directional Connectedness, $h = 1$ Month, by Country
48-month rolling window. Blue: lower tail ($\tau = 0.05$). Green: median ($\tau = 0.50$). Red: upper tail ($\tau = 0.95$). Positive values indicate net transmitter, negative values net receiver. Shaded bands mark the major stress episodes discussed in the text. Source: own calculations.

5.3.5 The horizon dimension

The horizon comparison in Table 6 and Figure 11 shows that the network's architecture is at least as sensitive to the forecast horizon as it is to the quantile. Two patterns stand out beyond the Nicaragua reversal already discussed. Panama moves from the system's largest net receiver at $h = 1$, upper tail (NET $= -46.6$), to a net transmitter at $h = 3$ (NET $= +29.0$) before returning to a receiver role at $h = 12$ (NET $= -33.8$), a non-monotonic pattern that suggests its tail-specific exposure operates on a different clock than the other economies, plausibly reflecting the mixed influence of short-run trade-and-logistics shocks against longer-run financial-sector conditions. Guatemala transitions from a mild net receiver at $h = 1$ upper tail (NET $= +2.5$, essentially neutral) to a more clearly negative position at $h = 3$ (NET $= -13.4$) and $h = 12$ (NET $= -4.6$), a pattern broadly consistent with the growing external-accounts share of its uncertainty composition documented in Figure 2, since external shocks of the kind that show up in that category plausibly take more than one month to work through the economy. These horizon-sensitive role changes are, again, reduced-form regularities in this sample. They describe how the estimated network reorganises itself across forecast horizons. They do not identify the economic channel responsible for any single country's shift.

5.4 Tier 3: Verification Exercises

Two features of the results above warrant dedicated scrutiny before they are treated as stable empirical regularities, the reliability of the tail amplification magnitude given estimation uncertainty, and the possibility that a common global factor, rather than genuine cross-country transmission, mechanically generates high connectedness at the upper tail. To probe both, we implement an independent, equation-by-equation quantile-VAR and generalised-FEVD estimator in R, following the same construction as Chatziantoniou et al. (2021), coded separately from the main estimation pipeline and used exclusively for the two checks below. This independent estimator reproduces the qualitative pattern of the main results, an upper-tail TCI well above the median and the United States as the dominant net transmitter, though not their exact magnitudes, reflecting differences in implementation detail between the two codebases. The checks below should be read as evidence about the direction and stability of the paper's central claims rather than as a re-estimate of the headline numbers in Tables 6 through 8.

5.4.1 Is the tail amplification distinguishable from sampling noise?

We construct a stationary block bootstrap, with 24-month blocks and 150 resamples, around the independent QVAR-GFEVD estimator, at $h = 1$, for both $\tau = 0.50$ and $\tau = 0.95$. The resulting 95 % confidence intervals are [38.5, 56.9] for the median TCI and [62.8, 87.1] for the upper-tail TCI. The two intervals are clearly separated, with a

gap of nearly six percentage points between the upper bound of the median interval and the lower bound of the upper-tail interval, indicating that the tail-amplification finding is unlikely to be an artefact of sampling variation in this specification. Given that this check uses an independently coded estimator rather than the main estimation pipeline, the appropriate conclusion is that the amplification survives a basic robustness test, not that its exact magnitude has been independently confirmed to three significant figures.

5.4.2 Is the upper-tail TCI a mechanical consequence of a shared US factor?

If all eight MUI series load heavily on a common global factor, proxied here by contemporaneous US uncertainty itself, then a high upper-tail TCI could arise mechanically from shared factor exposure rather than from genuine bilateral or regional transmission. To assess this, we orthogonalise each CAPRD country's MUI with respect to contemporaneous US MUI, regressing each series on US MUI and retaining the residual, recentred at the original country mean, and re-estimate the $\tau = 0.95$, $h = 1$ connectedness network on the orthogonalised system using the same independent estimator. The upper-tail TCI falls from 75.1 % in the raw, independent-estimator baseline to 74.0 %, a retention of 98.6 % of its original magnitude. Purging each CAPRD economy's uncertainty of its contemporaneous linear association with US uncertainty removes only a small fraction of the estimated connectedness, indicating that the tail amplification documented in this paper is not primarily a mechanical consequence of common US factor loading. This does not rule out that a broader global factor, encompassing for instance global risk sentiment beyond what US MUI alone captures, contributes to part of the remaining connectedness, a question this paper leaves for future work.

6 Discussion

Read together, the three tiers of results support a specific and fairly narrow set of empirical claims about the CAPRD uncertainty network over 1995 to 2025, and it is worth being explicit about the basis for each.

The data support, first, that the CAPRD uncertainty network is regime-dependent in a way that a conventional, mean-based connectedness analysis would not detect. Our QVAR estimates show total connectedness rising from 26.5 % at the median to 94.0 % at the upper tail at a one-month horizon, and from 17.1 % to 71.2 % at a twelve-month horizon. This pattern echoes, in a new geographic setting, the finding of Chatziantoniou et al. (2021) for interest-rate swaps and of Ben Haddad et al. (2024) for disaggregated JLN sub-indices, and is broadly consistent with the theoretical premise, traced through Bloom (2009) and Bloom (2014), that the real consequences of uncertainty concentrate in its tails. The data support, second, a specific and asymmetric network architecture at the upper tail, with the United States and Honduras as systematic net transmitters, Panama and the Dominican Republic as systematic net receivers at short horizons, Costa Rica as a net receiver almost everywhere in the specification space, and a network density among CAPRD economies themselves that goes beyond what a simple relay of US shocks would produce. This contrasts with the picture in Gabauer and Gupta (2018) and Antonakakis et al. (2018) of the United States as an overwhelmingly dominant hub among developed economies. In the CAPRD, the United States is dominant but not alone, and Honduras's transmitter role in particular is not straightforwardly predicted by economic size, in contrast to the size-weighted intuition that a reader might carry over from the regional integration literature of Urbina and Marenco (2024). The data support, third, that this architecture reorganises itself across the forecast horizon in ways that carry real economic content rather than representing estimation noise. Nicaragua's transition from a modest net receiver at $h = 1$ to the system's second-largest net transmitter at $h = 12$, upper tail, is the clearest instance of this reorganisation, and Panama's non-monotonic path across horizons is a second.

What the orthogonalisation exercise adds to this picture is a partial answer to an obvious objection. A reader might suspect that a network in which the United States dominates and in which upper-tail connectedness is uniformly high simply reflects the fact that all eight economies are exposed to the same US-driven global cycle, so that the appearance of a rich regional network is really an artefact of a single common factor. The finding that upper-tail connectedness retains 98.6 % of its magnitude after purging each CAPRD MUI of its linear association with contemporaneous US uncertainty speaks directly against that reading. Whatever generates the dense upper-tail network documented in Section 5.3.3, it is not simply a shared loading on US conditions.

The Nicaragua finding deserves a separate comment, because it is the result most likely to prompt a structural question a reduced-form QVAR cannot answer on its own. The finding that Nicaragua's uncertainty becomes a leading regional transmitter specifically at long horizons and during acute stress is consistent with several non-competing stories, including genuine trade or remittance-based propagation, shared exposure to Central American climate and security shocks that reach Nicaragua with a lag, or simply that Nicaraguan uncertainty is an informative slow-moving indicator of a regional shock that originates elsewhere and accumulates in Nicaragua's own uncertainty measure before it does elsewhere. The QVAR framework, by construction, cannot adjudicate between these readings. The same caveat applies to Guatemala's large transient upper-tail spikes between 2015 and 2022, whose magnitude and timing Figure 12 documents clearly but whose structural source remains outside what this paper's methodology can identify.

Prior work by Diakonova et al. (2025), Molina et al. (2023), McLean et al. (2024), McLean (2026), and Urbina and Marenco (2024) has already documented uncertainty, inflation spillovers, EPU transmission from the United States and China, and integration dynamics within the bloc using EPU-style proxies and mean-based or Bayesian VAR methods. McLean (2026) in particular already shows, at the mean, that US EPU dominates bilateral transmission into most CAPRD economies while China's influence is more diffuse and system-wide, a finding this paper's own result on US dominance at the upper tail of MUI connectedness echoes and sharpens by showing that the same US-centred asymmetry not only holds at the mean but strengthens considerably under stress. The contribution here is to construct a theoretically disciplined JLN-style uncertainty measure for all eight economies on a common thirty-year sample and to show that the resulting cross-country network is not adequately summarised by its conditional-mean behaviour. Whether the same amplification pattern generalises to other small-open-economy blocs, or is specific to the particular trade, remittance, and dollarisation structure of the CAPRD, is an open question that a single-region study cannot answer on its own.

7 Conclusion

This paper constructs country-specific macroeconomic uncertainty indices for the seven CAPRD economies and the United States following Jurado et al. (2015), and estimates the cross-country quantile connectedness network following Chatziantoniou et al. (2021) over 1995:05 to 2025:12. Three findings summarise the paper's empirical content. Our QVAR estimates show that cross-border uncertainty connectedness in the CAPRD network expands from 26.5 % of forecast error variance at the median to 94.0 % at the upper tail at a one-month horizon, and that a comparable amplification holds at three-month and twelve-month horizons. Our static and dynamic connectedness estimates identify the United States and Honduras as the region's most consistent net transmitters of uncertainty and Panama and the Dominican Republic as its most consistent net receivers at short horizons, an architecture that is denser and less US-centric than a simple hub-and-spoke reading would suggest. Our horizon comparison documents a marked reorganisation of the network at longer horizons, most notably Nicaragua's emergence as the system's second-largest net transmitter at $h = 12$, upper tail, a role it does not hold at shorter horizons, and this reorganisation survives an independent verification exercise built around a separately coded quantile-VAR estimator.

These are findings about the estimated statistical structure of uncertainty transmission in this sample, for this set of countries, over this period, using this method. They document tail dependence and an asymmetric, horizon-sensitive network architecture. They do not identify a structural transmission mechanism, and they carry no direct policy implication about how any central bank or government should respond to an uncertainty shock. What they offer is a disciplined empirical baseline, a full quantile-connectedness network estimated for this specific eight-economy uncertainty system, against which future work using higher-frequency data, structural identification, or an expanded sample as the post-2025 period accumulates further observations can be compared. The most promising next steps that follow directly from the results are a structural investigation of Nicaragua's long-horizon transmitter role, using country-level trade and remittance data to test which channel best accounts for its emergence, and an extension of the orthogonalisation exercise in Section 5.4 to a broader set of global factors beyond US uncertainty alone. A further natural extension is methodological rather than substantive, the quantile-on-quantile connectedness measures recently proposed by Gabauer and Stenfors (2024) would let a future study ask not only whether transmission intensifies when the *receiving* country is in its own upper tail, as the symmetric quantile design of Chatziantoniou et al. (2021) used throughout this paper implicitly assumes, but whether the transmitting and receiving quantiles need not coincide, a distinction that could matter given how much the network's architecture already changes across the horizon and quantile dimensions documented here.

A Appendix: MUI Construction Data

Table 9 reports the number of series entering each country's macroeconomic uncertainty panel by economic category, prior to the factor-augmented stochastic volatility estimation described in Section 3. These counts are the underlying data referenced in Section 4 and in Figure 2.

Table 9: Number of Series by Category in Each Country's MUI Estimation Panel

Category	CRI	DOM	GTM	HND	NIC	PAN	SLV	Total
Activity	42	1	14	12	15	1	18	103
Prices	31	13	15	13	40	55	42	209
Money	4	29	8	25	9	5	22	102
Banking	10	29	14	7	4	16	10	90
Public Sector	20	6	9	6	20	7	9	77
External	8	15	74	42	13	6	11	169
Interest Rates	2	10	5	8	11	22	14	72
FX and Risk	2	4	2	1	4	0	0	13
Labor	0	0	0	0	12	0	0	12
Climate	0	0	0	0	1	0	0	1
Energy	0	0	0	0	4	0	0	4
Total panel size	**119**	**107**	**141**	**114**	**133**	**112**	**126**	

Source: country-level MUI construction panels (own data collection and compilation). Each series is assigned a stationarity-inducing transformation code (level, Δlevel, Δ^2level, log, Δlog, Δ^2log) and, where flagged, seasonally adjusted prior to transformation, following the pipeline in Section 3. United States panel constructed separately from a comparable US-specific data source and omitted here for space; its category composition is available on request.

Figures 13 through 15 provide the chord-diagram counterpart to the thresholded network graphs in Figures 7 through 9, showing the full gross pairwise contribution between every pair of economies without any thresholding and without any own-shock (diagonal) ribbon.

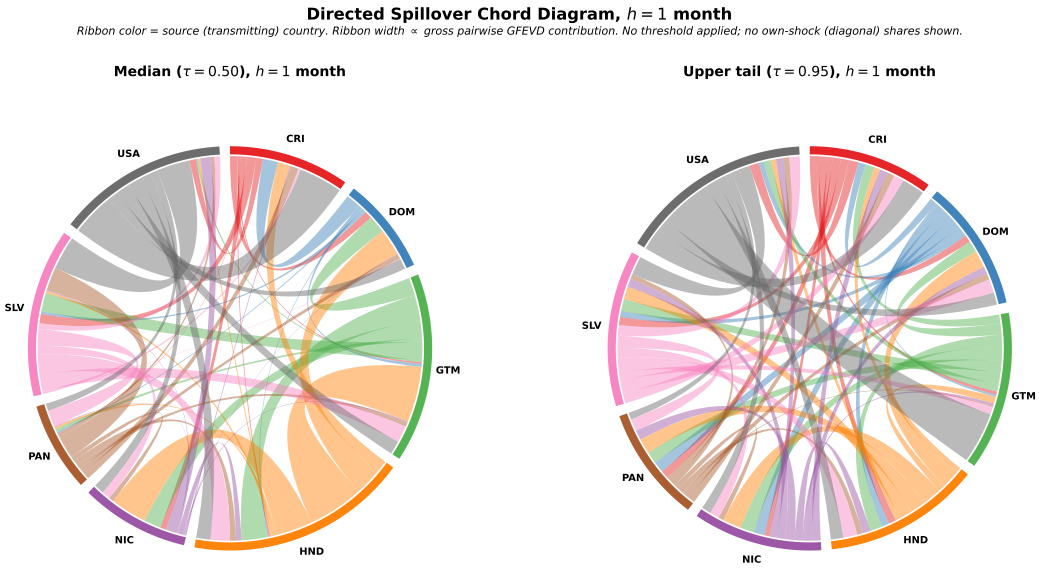


Figure 13: Directed Spillover Chord Diagram, $h = 1$ Month
Left: median ($\tau = 0.50$). Right: upper tail ($\tau = 0.95$). Ribbon colour identifies the source (transmitting) country; ribbon width is proportional to the gross pairwise GFEVD contribution from that source to the receiving country. No threshold is applied and no own-shock share is shown, so this figure gives the complete pairwise detail underlying Figure 7. Data: 1995:05 to 2025:12; QVAR($p = 2$), nfore = 12, corrected GFEVD. Source: own calculations.

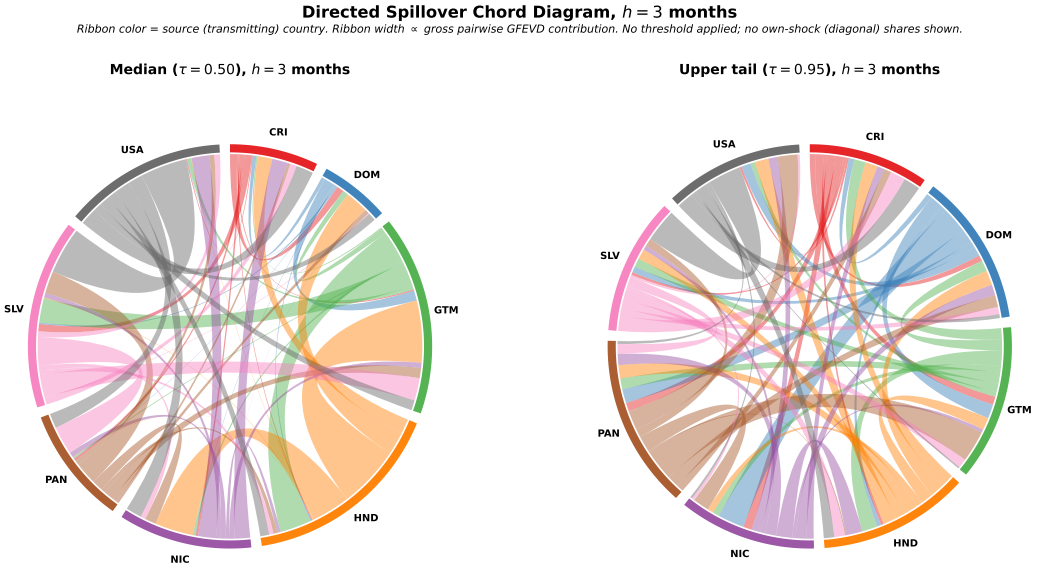


Figure 14: Directed Spillover Chord Diagram, $h = 3$ Months
Same conventions as Figure 13.

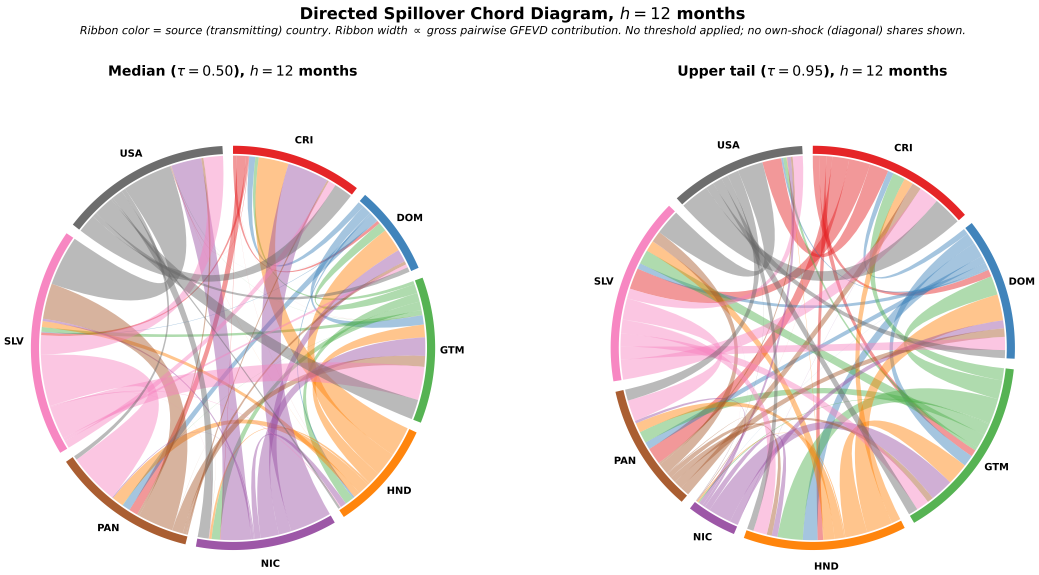


Figure 15: Directed Spillover Chord Diagram, $h = 12$ Months
Same conventions as Figure 13.

A.1 Additional Country-Level VAR Impulse Responses

Figures 16 through 20 report the recursive VAR impulse responses to a domestic uncertainty shock for the five CAPRD economies discussed but not shown in Section 5.2.1, using the same identification strategy and confidence bands as Figures 4 and 5, with the variable set in each panel tailored to that country's monetary regime and data availability as described in the main text.

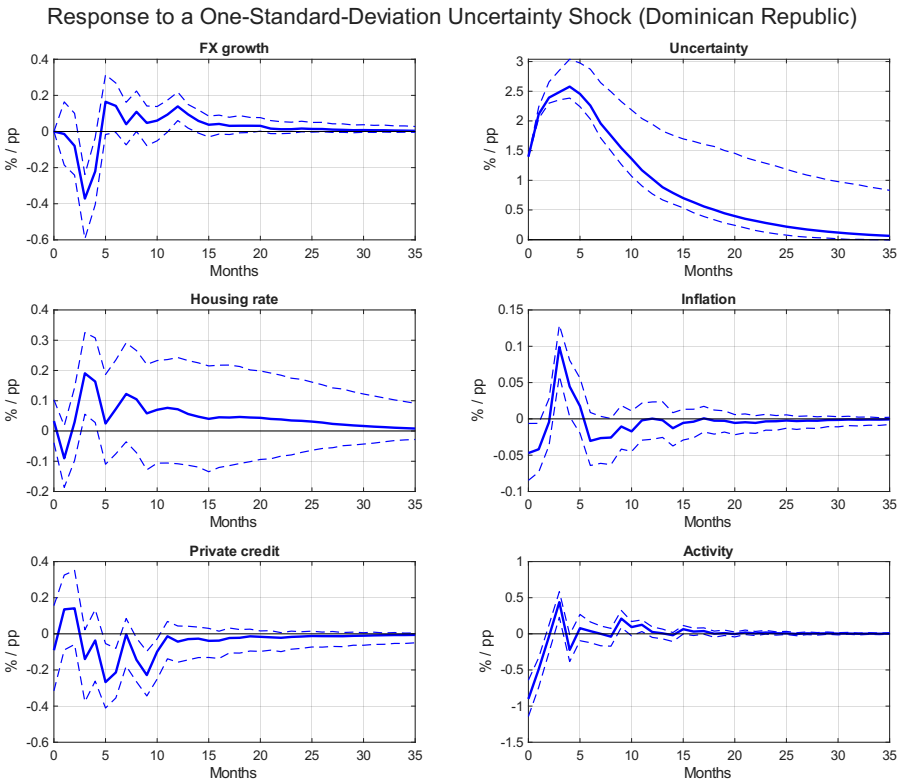


Figure 16: Response to a One-Standard-Deviation Uncertainty Shock, Dominican Republic
Same conventions as Figure 4.

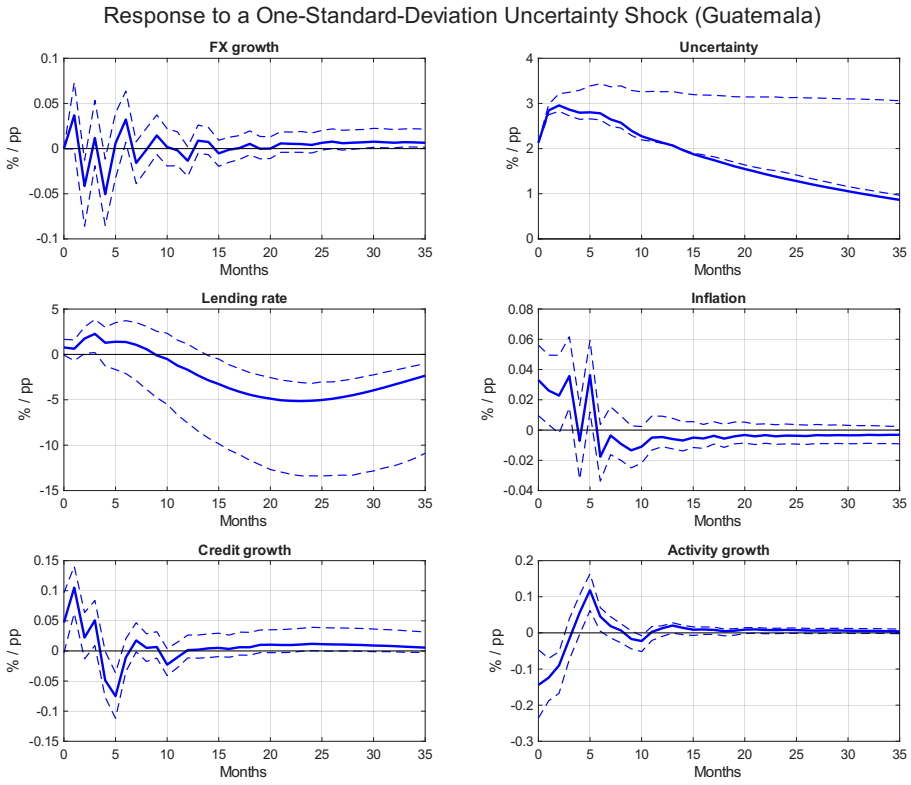


Figure 17: Response to a One-Standard-Deviation Uncertainty Shock, Guatemala
Same conventions as Figure 4.

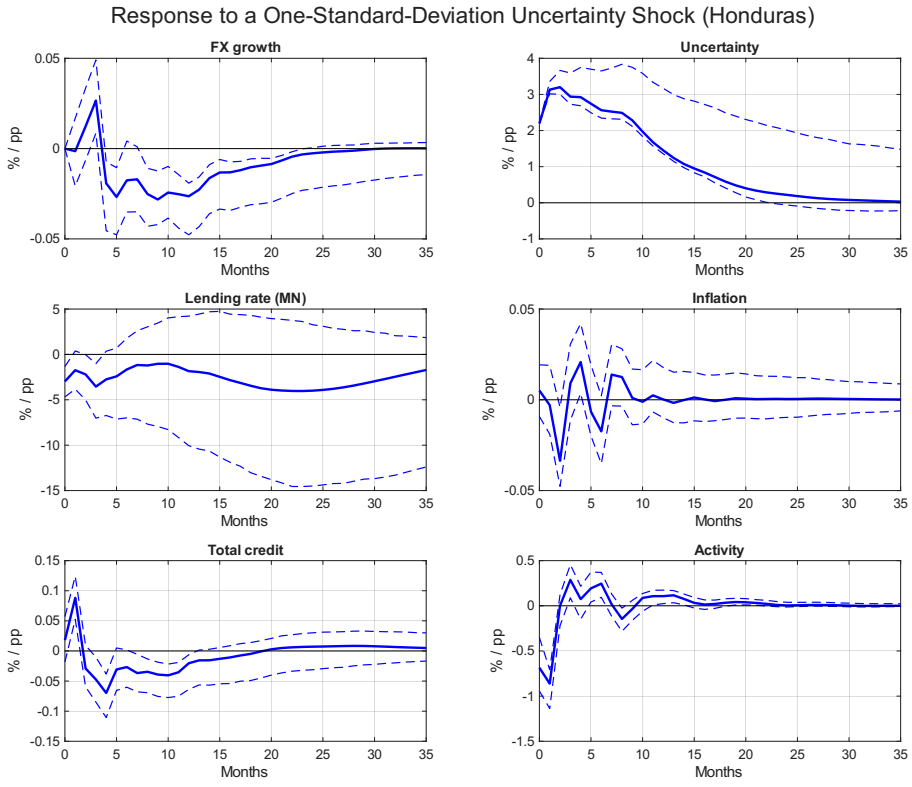


Figure 18: Response to a One-Standard-Deviation Uncertainty Shock, Honduras
Same conventions as Figure 4.

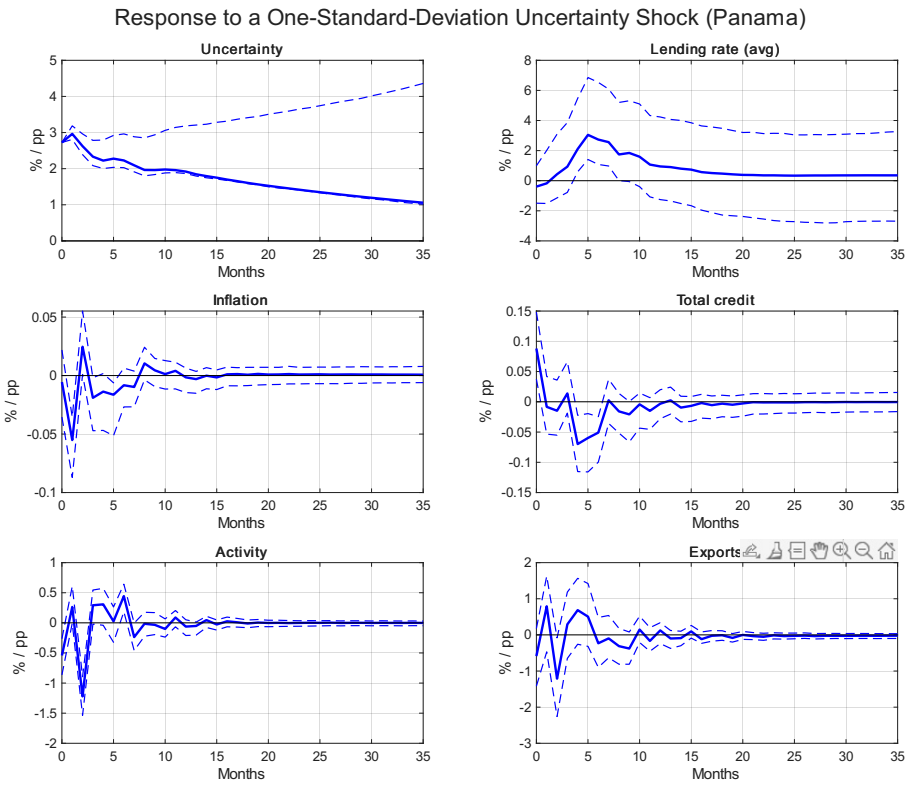


Figure 19: Response to a One-Standard-Deviation Uncertainty Shock, Panama
Same conventions as Figure 4.

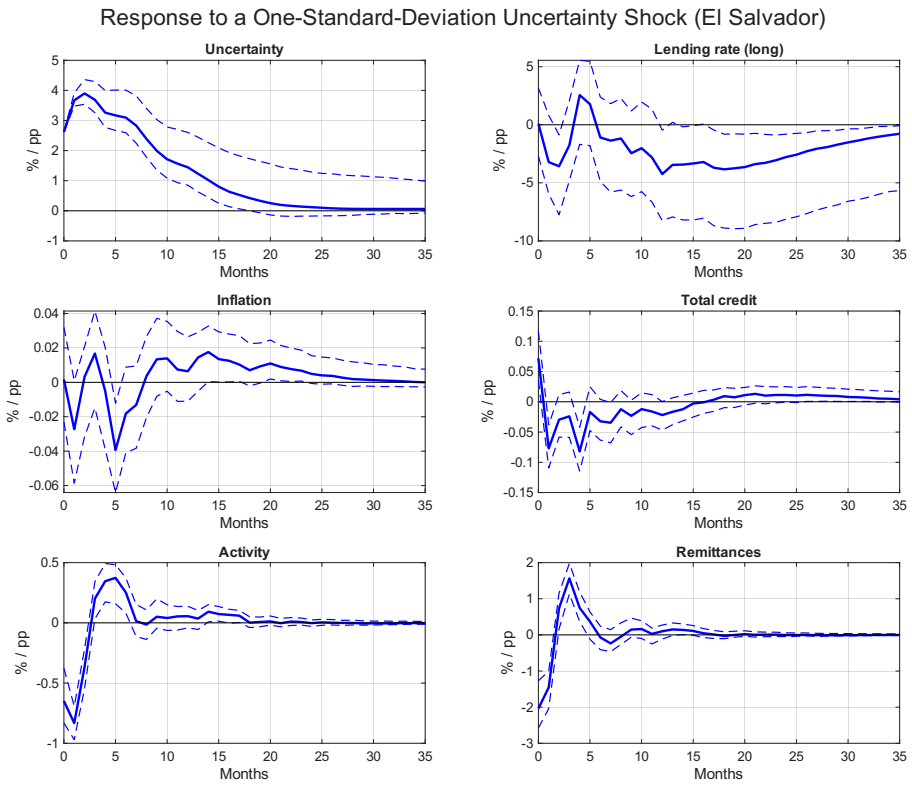


Figure 20: Response to a One-Standard-Deviation Uncertainty Shock, El Salvador
Same conventions as Figure 4.

References

Ahir, H., Bloom, N., and Furceri, D. (2022). The world uncertainty index. Technical Report 29763, National Bureau of Economic Research.

Andres-Escayola, E., Molina, L., Pérez, J. J., and Vidal, E. (2025). How economic policy uncertainty spreads across borders: The case of Latin America. Working Paper 2549, Banco de España.

Antonakakis, N., Gabauer, D., Gupta, R., and Plakandaras, V. (2018). Dynamic connectedness of uncertainty across developed economies: A time-varying approach. *Economics Letters*, 166:63–75.

Backus, D. K. and Zin, S. E. (1994). Reverse engineering the yield curve. Technical Report 4676, National Bureau of Economic Research. National Bureau of Economic Research.

Bai, J. and Ng, S. (2002). Determining the number of factors in approximate factor models. *Econometrica*, 70(1):191–221.

Baker, S. R., Bloom, N., and Davis, S. J. (2016). Measuring economic policy uncertainty. *The Quarterly Journal of Economics*, 131(4):1593–1636.

Ben Haddad, H., Mezghani, I., Medhioub, I., and Altamimi, S. (2024). Spillover effects of disaggregated macroeconomic uncertainties on U.S. real activity: Evidence from the quantile vector autoregressive connectedness approach. *Empirical Economics*, 66(2):829–858.

Biljanovska, N., Grigoli, F., and Hengge, M. (2021). Fear thy neighbor: Spillovers from economic policy uncertainty. *Review of International Economics*, 29(2):409–438.

Bloom, N. (2009). The impact of uncertainty shocks. *Econometrica*, 77(3):623–685.

Bloom, N. (2014). Fluctuations in uncertainty. *Journal of Economic Perspectives*, 28(2):153–176.

Bloom, N., Bond, S., and Van Reenen, J. (2007). Uncertainty and investment dynamics. *Review of Economic Studies*, 74(2):391–415.

Calderón, C. and Fuentes, J. A. (2014). Have business cycles changed over the last two decades? an empirical investigation. *Journal of Development Economics*, 109:98–123.

Cascaldi-Garcia, D., Sarisoy, C., Londono, J. M., Sun, B., Datta, D. D., Ferreira, T., Grishchenko, O., Jahan-Parvar, M. R., Loria, F., Ma, S., Rodriguez, M., Zer, I., and Rogers, J. H. (2023). What is certain about uncertainty? *Journal of Economic Literature*, 61(2):624–654.

Chatziantoniou, I., Gabauer, D., and Stenfors, A. (2021). Interest rate swaps and the transmission mechanism of monetary policy: A quantile connectedness approach. *Economics Letters*, 204:109891.

Diakonova, M., Ghirelli, C., and Juan Quiñónez Wu (2025). Economic policy uncertainty in Central America and the Dominican Republic. *Latin American Journal of Central Banking*, 7(2).

Diakonova, M., Molina, L., Mueller, H., Pérez, J. J., and Rauh, C. (2024). The information content of conflict, social unrest and policy uncertainty measures for macroeconomic forecasting. *Latin American Journal of Central Banking*, 5(4):100130.

Dickey, D. A. and Fuller, W. A. (1979). Distribution of the estimators for autoregressive time series with a unit root. *Journal of the American Statistical Association*, 74(366):427–431.

Diebold, F. X. and Yilmaz, K. (2009). Measuring financial asset return and volatility spillovers, with application to global equity markets. *Economic Journal*, 119(534):158–171.

Diebold, F. X. and Yilmaz, K. (2012). Better to give than to receive: Predictive directional measurement of volatility spillovers. *International Journal of Forecasting*, 28(1):57–66.

Diebold, F. X. and Yilmaz, K. (2014). On the network topology of variance decompositions: Measuring the connectedness of financial firms. *Journal of Econometrics*, 182(1):119–134.

Elliott, G., Rothenberg, T. J., and Stock, J. H. (1996). Efficient tests for an autoregressive unit root. *Econometrica*, 64(4):813–836.

Fernández-Villaverde, J., Guerrón-Quintana, P., Kuester, K., and Rubio-Ramírez, J. (2015). Fiscal volatility shocks and economic activity. *American Economic Review*, 105(11):3352–3384.

Gabauer, D. (2022). ConnectednessApproach: Connectedness Approach (r package version 1.0.2). Available at https://CRAN.R-project.org/package=ConnectednessApproach.

Gabauer, D. and Gupta, R. (2018). On the transmission mechanism of country-specific and international economic uncertainty spillovers: Evidence from a TVP-VAR connectedness decomposition approach. *Economics Letters*, 171:63–71.

Gabauer, D. and Stenfors, A. (2024). Quantile-on-quantile connectedness measures: Evidence from the US treasury yield curve. *Finance Research Letters*, 60:104866.

Ghirelli, C., Pérez, J. J., and Urtasun, A. (2020). Economic policy uncertainty in Latin America: Measurement using Spanish newspapers and economic spillovers. Working Paper 2024, Banco de España.

Ghirelli, C., Pérez, J. J., and Urtasun, A. (2021). The spillover effects of economic policy uncertainty in Latin America on the Spanish economy. *Latin American Journal of Central Banking*, 2(2):100029.

International Monetary Fund (2022). Spillovers of US monetary tightening to latin America. In *Regional Economic Outlook: Western Hemisphere, October 2022*. International Monetary Fund, Washington, D.C. Background Paper 1.

International Monetary Fund (2024). Spillover effects of US monetary policy on emerging markets amidst uncertainty. Working Paper WP/24/04, International Monetary Fund, Washington, D.C.

Jarque, C. M. and Bera, A. K. (1980). Efficient tests for normality, homoscedasticity and serial independence of regression residuals. *Economics Letters*, 6(3):255–259.

Jurado, K., Ludvigson, S. C., and Ng, S. (2015). Measuring uncertainty. *American Economic Review*, 105(3):1177–1216.

Jurado, K., Ludvigson, S. C., and Ng, S. (2024). JLN macroeconomic uncertainty indexes. Data series, Federal Reserve Bank of St. Louis (FRED). Series JLNUM1M, JLNUM3M, JLNUM12M. Retrieved July 2025.

Kastner, G. (2016). Dealing with stochastic volatility in time series using the R package `stochvol`. *Journal of Statistical Software*, 69(5):1–30.

Knight, F. H. (1921). *Risk, Uncertainty and Profit*. Houghton Mifflin, Boston.

Koenker, R. and Bassett, G. (1978a). Regression quantiles. *Econometrica*, 46(1):33–50.

Koenker, R. and Bassett, G. (1978b). Regression quantiles. *Econometrica*, 46(1):33–50.

Koop, G., Pesaran, M. H., and Potter, S. M. (1996). Impulse response analysis in nonlinear multivariate models. *Journal of Econometrics*, 74(1):119–147.

Kwiatkowski, D., Phillips, P. C. B., Schmidt, P., and Shin, Y. (1992). Testing the null hypothesis of stationarity against the alternative of a unit root. *Journal of Econometrics*, 54(1–3):159–178.

Ludvigson, S. C., Ma, S., and Ng, S. (2021). Uncertainty and business cycles: Exogenous impulse or endogenous response? *American Economic Journal: Macroeconomics*, 13(4):369–410.

McLean, R. (2026). Economic policy uncertainty spillovers from the United States and

China to Central American economies: A BGVAR approach. *Revista Económica de Centroamérica y República Dominicana (RECARD)*, 7(1).

McLean, R., Balladares, H., and Guerrero, J. (2024). Shocks globales y spillovers inflacionarios en Centroamérica y República Dominicana. *Revista Económica de Centroamérica y República Dominicana (RECARD)*, 5(1).

Molina, L., Pérez, J., Vidal, E., and Bykova, A. (2023). Political uncertainty in Latin America: A textual analysis. *Latin American Journal of Central Banking*, 4(4):100094.

Pesaran, M. H. (2004). General diagnostic tests for cross section dependence in panels. *Cambridge Working Papers in Economics*, 0435. Faculty of Economics, University of Cambridge.

Pesaran, M. H. and Shin, Y. (1998). Generalized impulse response analysis in linear multivariate models. *Economics Letters*, 58(1):17–29.

Phillips, P. C. B. and Perron, P. (1988). Testing for a unit root in time series regression. *Biometrika*, 75(2):335–346.

Pindyck, R. S. (1991). Irreversibility, uncertainty, and investment. *NBER Working Paper*, (3307).

Rossi, B. and Sekhposyan, T. (2015). Macroeconomic uncertainty indices based on nowcast and forecast error distributions. *American Economic Review*, 105(5):650–655.

Stock, J. H. and Watson, M. W. (2002). Forecasting using principal components from a large number of predictors. *Journal of the American Statistical Association*, 97(460):1167–1179.

Urbina, J. (2013). Financial spillovers across countries: Measuring shock transmissions. MPRA Paper 75756, University Library of Munich, Germany.

Urbina, J. and Marenco, M. (2024). Midiendo el grado de integración económica centroamericana vía dinámica de interconectividad y spillovers. *Revista de Fomento Social*, 79(309):321–339.

Wickham, H. (2016). *ggplot2: Elegant Graphics for Data Analysis*. Springer-Verlag, New York.